DR JÖRG KRUSE (Orcid ID : 0000-0002-5007-7722)

PROF. JOERG-PETER SCHNITZLER (Orcid ID : 0000-0002-9825-867X)

Article type : Regular Article

Optimization of photosynthesis and stomatal conductance in the date palm *Phoenix dactylifera* during acclimation to heat and drought

Jörg Kruse[1,4,7], Mark Adams[4,5], Barbro Winkler[2], Andrea Ghirardo[2], Saleh Alfarraj[3], Jürgen Kreuzwieser[1], Rainer Hedrich[6], Jörg-Peter Schnitzler[2] & Heinz Rennenberg[1,3]

[1]Institute of Forest Sciences, Chair of Tree Physiology, University of Freiburg, Georges-Köhler-Allee 53/54, 79110 Freiburg, Germany

[2]Research Unit Environmental Simulation, Institute of Biochemical Plant Pathology, Helmholtz Zentrum München, 85764 Neuherberg, Germany

[3]College of Sciences, King Saud University, P.O. Box 2455, Riyadh 11451, Saudi Arabia

[4]Faculty of Agriculture and Environment, University of Sydney, Sydney, NSW 2006, Australia.

[5]Swinburne University of Technology, John St, Hawthorn, Vic 3122, Australia

[6]Institute for Molecular Plant Physiology and Biophysics, Biocenter, University of Würzburg, 97082 Würzburg, Germany

[7]Corresponding author; E-mail: joerg.kruse@ctp.uni-freiburg.de; Tel: +49 (0)761 203-8300

This article has been accepted for publication and undergone full peer review but has not been through the copyediting, typesetting, pagination and proofreading process, which may lead to differences between this version and the Version of Record. Please cite this article as doi: 10.1111/nph.15923
This article is protected by copyright. All rights reserved.

Accepted Article

Accepted Article

Received: *19 January 2019*

Accepted: *1 May 2019*

Orcid:

Jörg Kruse: http://orcid.org/0000-0002-1614-8128

Mark Adams: http://orcid.org/0000-0001-8989-508X

Barbro Winkler: http://orcid.org/0000-0002-7092-9742

Andrea Ghirardo: http://orcid.org/0000-0003-1973-4007

Jürgen Kreuzwieser: http://orcid.org/0000-0002-5251-9723

Rainer Hedrich: http://orcid.org/0000-0003-3224-1362

Jörg-Peter Schnitzler: http://orcid.org/0000-0002-9825-867X

Heinz Rennenberg: http://orcid.org/0000-0001-6224-2927

Summary

- We studied acclimation of leaf gas exchange to differing seasonal climate and soil water availability in slow- growing date palm seedlings (*Phoenix dactylifera*). We used an extended Arrhenius-equation to describe instantaneous temperature responses of leaf net photosynthesis (*A*) and stomatal conductance (*G*), and derived physiological parameters suitable for characterization of acclimation (T_{opt}, A_{opt} and T_{equ}).
- Optimum temperature of *A* (T_{opt}) ranged between 20 -33°C in winter and 28 -45°C in summer. Growth temperature (T_{growth}) explained ~50% of the variation in T_{opt}, which additionally depended on leaf water status at the time- of- measurement. During

This article is protected by copyright. All rights reserved.

Accepted Article

water-stress, light - saturated rates of *A* at T_{opt} (i.e, A_{opt}) were reduced to 30-80% of control levels, albeit not limited by CO_2- supply *per se*.

- Equilibrium temperature (T_{equ}), around which *A*/*G* and substomatal [CO_2] are constant, remained tightly coupled with T_{opt}. Our results suggest that acclimatory shifts in T_{opt} and A_{opt} reflect a balance between maximization of photosynthesis whilst minimizing the risk of metabolic perturbations caused by imbalances in cellular [CO_2].
- This novel perspective on acclimation of leaf gas exchange is compatible with optimization theory, and might help elucidating other acclimation and growth strategies in species adapted to differing climates.

Keywords: Acclimation, adaptation, Arrhenius equation, flux control, temperature response, stomata, water use efficiency (WUE).

1. Introduction

Loss of water vapor is an inevitable consequence of carbon fixation in C_3- photosynthesis. Long-term selection pressures have mostly ensured that stomatal aperture is controlled such that loss is minimized (Cowan 1977, Farquhar & Sharkey 1982). Over shorter time periods, adaptation to specific site conditions and climate is also reflected in control of leaf gas exchange. Here, sub-stomatal CO_2- concentration (C_i) is a signal (Assmann 1999) for adjustment of stomatal aperture such that inward CO_2- diffusion can meet the CO_2- demand. At near- constant ambient temperature, for example, responses of net photosynthesis (*A*; μmol CO_2 m^{-2} s^{-1}) and stomatal conductance (*G*; mmol H_2O m^{-2} s^{-1}) are largely proportional to short- term changes in incident light (Wong *et al.* 1985, Mott 1988), and photosynthetic water use efficiency (*A*/*G*; μmol mol^{-1}) and C_i remain constant. At constant irradiance, by

This article is protected by copyright. All rights reserved.

contrast, short- term shifts in ambient (measurement) temperature are associated with changing relative humidity and can disrupt the linear relationship between *A* and *G* (Wong *et al.* 1979, Aphalo & Jarvis 1991, Lin *et al.* 2012). Consequently, C_i typically varies with measurement temperature. This is due to: **(1)** the strong temperature dependence of biochemical reactions that comprise the Calvin-cycle, and **(2)** the additional sensitivity of guard cells that help regulate *G* to humidity (or leaf-to-air vapor pressure deficit; Ball, Woodrow & Berry 1987, Leuning 1995, Oren *et al.* 1999), and hence transpiration (Mott & Parkhurst 1991, Eamus *et al.* 2008).

The temperature dependency of photosynthesis (*A*) can be described by an extended Arrhenius equation (Kruse *et al.* 2017a, b). Variation in Arrhenius-type parameters mostly depends on legacies of past environmental conditions (Kruse, Turnbull & Adams 2012). Such 'memory effects' define leaf metabolic state at the onset of any new condition(s) and are the basis of the present acclimation study. Arrhenius-type parameters also vary between species, reflecting adaptation or 'evolutionary memory' to preferred habitats (Kruse, Turnbull & Adams 2012). Exploration of this variation seems likely to improve the mechanistic understanding of *in vivo* flux control at the time of measurement, and species- specific acclimation strategies to changing growth temperature or soil water availability (i.e., Silim *et al.* 2010, Rogers *et al.* 2017). Amongst Arrhenius- type parameters, exploration of acclimatory shifts in δ- parameter is of particular importance (see Equation 2 in Section 2.3). For $\delta = 0$, rates of reaction strictly follow 'classical' Arrhenius- kinetics and increase exponentially with measurement temperature, as is frequently observed for leaf dark respiration (Joseph *et al.* 2014, Reich *et al.* 2016, Drake *et al.* 2016). By contrast, rates of leaf net photosynthesis show more pronounced curvature in response to measurement temperature, as defined by temperature- dependent decline in activation energy of *A* (i.e, δ_A).

This article is protected by copyright. All rights reserved.

Accepted Article

Consequently, leaf photosynthesis generally peaks at some distinct optimum temperature (T_{opt}) within physiologically relevant temperature ranges (i.e., 10-40°C; Berry & Björkman 1980, Way & Yamori 2014).

Plants are capable to physiologically adjust T_{opt} to changes in leaf temperature, such that photosynthesis can be maximized irrespective of variation in ambient temperature. Optimal regulation of stomatal aperture should allow for maximizing carbon gain (*A*) whilst minimizing transpirational water loss (*E*) over a certain period of time (Cowan & Farquhar 1977, Medlyn *et al.* 2011). Physiological mechanisms conferring this kind of stomatal behavior remain elusive, but might be approachable by taking a different view on putatively 'optimal' coordination between *A* and *G*. It is conceivable, but has to our knowledge not been tested experimentally, that such coordination ensures temperature- dependent variation in C_i is minimized proximal to T_{opt}. In this way, photosynthetic performance at T_{opt} (i.e., A_{opt}, µmol m^{-2} s^{-1}) could be stabilized, in order to avoid imbalances in CO_2- supply and CO_2-demand that might otherwise cause generation of harmful reactive oxygen species (ROS; Rennenberg *et al.* 2006, Lawlor & Tezara 2009).

The leaf temperature, at which C_i is most insensitive to temperature variation, can be defined via application of the extended Arrhenius- approach to both *A* and *G* (see section 2.3), and has been dubbed 'equilibrium temperature' (T_{equ}). Acclimation of T_{equ} to growth temperature (and air humidity) or declining soil water availability could provide new information about coordination of *A* and *G* (Quick *et al.* 1992, Medrano *et al.* 2002, Lawlor 2002). For example, midday depression of CO_2-assimilation on a clear, sunny day has often been ascribed to stomatal closure, causing a drop in C_i that limits light-saturated photosynthesis (Raschke &

This article is protected by copyright. All rights reserved.

Accepted Article

Reeseman 1986, Macfarlane *et al.* 2004). But it remains difficult to distinguish between cause and effect, giving rise to co- variation between C_i, *G* and *A* (Lawlor & Cornic 2002). There is an ongoing and often vigorous debate, whether drought initiates photosynthetic down-regulation *via* stomatal closure (Boyer 1976, Schulze 1986, Cornic 2000, Flexas & Medrano 2002), or *via* a decline of 'mesophyll capacity' (Tezara *et al.* 1999, Chaves *et al.* 2009, Damour *et al.* 2009, Lawlor & Tezara 2009).

In the present study, we explored acclimation of leaf gas exchange in date palm seedlings (*Phoenix dactylifera*). Date palm is adapted to hot and semi-arid environments, with centers of cultivation in the Middle East and the Maghreb countries of Northern Africa (Tengberg 2003). Gas exchange was analyzed with atmospheric conditions similar to those in Saudi Arabian winter and summer, with carefully controlled soil water deficits and recovery from the preceding drought period (Rennenberg *et al.* 2006). Our general aim was to characterize variation in Arrhenius- type parameters for both *A* and *G* during acclimation to heat, drought and recovery. Specifically, we tested the following hypotheses: (1) T_{opt} tracks changes in ambient temperature, in order to maximize *A* (i.e., $T_{opt} - T_{growth} = 0$). (2) T_{equ} remains closely coupled with T_{opt}, in order to minimize the risk of metabolic perturbation at maximum possible rate of *A* under treatment conditions (i.e., $T_{equ} - T_{opt} = 0$). (3) Drought causes over-proportional reduction in *G* and an increase in photosynthetic water use efficiency (WUE_i =A/G), indicating CO_2- source limitation of *A*. To test the latter hypothesis, gas exchange measurements were supplemented with $\delta^{13}C$-analyses in bulk leaf material.

This article is protected by copyright. All rights reserved.

Accepted Article

2. Materials and Methods

2.1. Plant material and experimental setup

A total of 240, two-year old seedlings of Date palm (*Phoenix dactilyfera*) were purchased from a commercial supplier ('Der Palmenmann', Bottrop, Germany). Two months before the start of the experiment, plants were repotted (3.3-liter pots). Pots were filled with a peat-soil - sand - mixture (3:1:7 v/v/v), to which *c.* 10 g of Osmocote fertilizer were added (16% N, 9% P_2O_5, 12% K_2O). Plants were grown under greenhouse conditions (photoperiod 12h day: 12h night, 25: 15 °C, 20: 30% rH) and irrigated once per week (*c.* 150-200 ml per pot). After two months, on 10th of January 2014, plants were transferred to four, fully automatized, climate-controlled walk-in growth chambers (Helmholtz Zentrum, Munich, Germany; supplementary information Fig. S1a).

Two chambers were assigned to explore summer conditions and two to winter conditions. Each of the four chambers was equipped with four growth cabinets, and each cabinet was capable of holding 15 plants (supplementary information, Fig. S1b). Two cabinets per chamber were assigned to water-deprivation while the other two remained well-watered.

Conditions in growth chambers were slowly adjusted to match typical climate conditions during 2003-2012 in Alahsa, Saudi-Arabia. Winter conditions were selected as those prevailing for the period 21.12.-21.03, while summer conditions were those for the period 21.06.-21.09. Average noon temperatures peaked at *c.* 40°C in summer and 25°C in winter. These temperature differences persisted during the night (Fig. 1a). Vapour pressure deficit varied with growth temperature and peaked at *c.* 6.8 kPa is summer and 2.5 kPa in winter

This article is protected by copyright. All rights reserved.

(Fig. 1b). In the summer treatment, the light period was four hours longer than for the winter treatment, but maximum irradiance was similar (i.e., photon flux density: 600 μmol m^{-2} s^{-1}; Fig. 1c; for technical reasons somewhat less than under natural conditions). Average precipitation in Alahsa, Saudi-Arabia, amounts to 0.3± 0.8 mm in summer (median 0.0 mm) and 35.5± 30 mm in winter (median 30.9 mm). Selected daytime climates in winter and summer were maintained throughout the experiment (supporting information, Fig. S2).

We increased rates of irrigation of summer treatments on January 22nd so that all plants had comparable soil water conditions (Fig. 2). Acclimation of gas exchange of well-watered plants to seasonal growth temperature variation was measured between January 27th and 31st (T1 period: 'Temperature acclimation'; Table S1).

The drought period commenced on February 10th, when irrigation was reduced to 50% of control levels in winter and summer (Table S1; Fig. 2). Effects of 'mild drought' on leaf gas exchange were measured 1-2 weeks later (T2 period), during which soil water contents (ML3 Thetaprobe, Delta-T, UK) were reduced to 12.5% in summer and 14.1% in winter compared to *c.* 21.7% under well-watered conditions (Fig. 2). Irrigation was further reduced on February 20th, so that between March 4th and 11th soil water contents were less than 5% in summer and 6 - 7% in winter compared to 18-22 % of controls in summer and winter (see Fig. 2, T3 period). Once measurements during drought treatments were completed, we restored rates of irrigation to those of the control treatments and measured responses during this recovery phase (T4 period; Table S1).

This article is protected by copyright. All rights reserved.

Accepted Article

2.2. Leaf nitrogen contents and δ^{13}-signatures

We measured aboveground fresh mass of plants (after T1, T3 and T4), and the dry mass to fresh mass ratio (DM: FM) of individual leaves used in gas exchange measurements at the end of each experimental period (T1-T4). For a subset of samples (i.e., after T1 and T3) we also determined leaf mass per area (LMA; g DM m^{-2}). For this purpose, leaves were photographed and leaf area was analyzed via photoshop (www.adobe.com.de).

Samples were dried for 3 days at 65°C for further analysis. 1.5-2.5 mg of dried, pulverized material was combusted in an elemental analyzer (NA 2500; CE Instruments, Milan, Italy) for total leaf-N analysis, coupled to an Isotope Ratio Mass Spectrometer (Delta Plus/Delta Plus XL; Finnigan MAT GmbH, Bremen, Germany) by a Conflo II/III interface (Thermo-Finnigan GmbH, Bremen, Germany) for ^{13}C analysis. Relative abundance of ^{13}C in bulk leaf material was expressed as relative deviation from the international standard (V-PDB), using the δ- notation:

$$\delta^{13}C = \left(\frac{R_{sample}}{R_{standard}} - 1\right) \times 1000 \quad (8)$$

Instrument precision for $\delta^{13}C$ was ±0.05‰. $\delta^{13}C$ in bulk leaf material was used as a proxy for WUE_i (Kruse *et al.* 2012).

2.3. Gas exchange measurements

Prior to each measurement campaign (T1-T4 periods), three plants per growth cabinet were chosen at random from each season and irrigation treatment. We then measured gas exchange in the morning (7:45am-11:00am), at midday (11:00am-14:15pm), and in the afternoon

This article is protected by copyright. All rights reserved.

(14:15-17:30pm). Measurements were randomized between two portable infrared gas analyzers (GFS 3000, Walz, Effeltrich, Germany). By the end of each measurement campaign (4 days for T1; 8 days for T2, T3 and T4), we had completed four independent replicates for each season, irrigation treatment and day time (supporting information, Dataset S1 and Notes S1).

Temperatures within growth chambers were monitored continuously. We recorded the prevalent air temperature prior to start of each measurement (T_{growth}; accuracy ± 0.2°C). Temperature responses of net photosynthesis and stomatal conductance were determined for fully expanded leaves at the base of each plant. Palm leaves were located within a 8 cm^2 cuvette and flushed with air at a rate of 700 µmol s^{-1}. We replaced cuvette gaskets after every third set of temperature response measurements. Temperature responses of gas exchange were determined in seven, 3°C-steps (21°C to 39°C cuvette air temperature) at ambient CO_2 (380-400 µmol mol^{-1}) and saturating light intensity (PAR: 1.500 µmol m^{-2} s^{-1}). At the first target temperature (21°C), measurements were recorded after 20 minutes of equilibration. After each subsequent temperature change, plants were allowed to equilibrate for 10 minutes. Gas exchange was then recorded and averaged over a period of 5 minutes (Kruse *et al.* 2017a, b). After the last measurement (at 39°C), the light source was turned off. We waited until dark respiration (R_{39}; µmol m^{-2} s^{-1}) had equilibrated, before measurements were recorded (5-minutes average).

We used Pt100 sensors to monitor temperature, adjusted using Peltier elements (accuracy ± 0.1°C after 3 min. equilibration). Gas exchange systems allowed for good regulation of humidity. Absolute humidity was set at 13000± 50 ppm H_2O, irrespective of cuvette

This article is protected by copyright. All rights reserved.

Accepted Article

temperature. Vapour pressure deficit (VPD) in the cuvette increased from 1.5± 0.1 kPa at 21°C to 6.5± 0.2 kPa at 39°C. Spans of measurement temperature and VPD were chosen to encompass respective ranges in growth chambers during the light period (Fig. 1a, b).

Rates of CO_2-assimilation were assessed relative to leaf, rather than cuvette (air) temperature. Leaf temperature was determined via a thermocouple touching the lower leaf surface (accuracy ± 0.1°C). The temperature dependency of photosynthesis (*A*) can be described by an extended Arrhenius equation (Kruse *et al.* 2017a, b):

$$A = A_{ref} \times e^{\left[\frac{E_o(Ref.A)}{\Re}\times\left(\frac{T-T_{ref}}{T\times T_{ref}}\right)+\delta_A\times\left(\frac{T-T_{ref}}{T\times T_{ref}}\right)^2\right]} \quad (1)$$

where T is the measurement temperature (K), T_{ref} is a reference temperature (294 K (= 21°C) in the present study), $\Re$ is the universal gas constant (8.314 J mol^{-1} K^{-1}), A_{ref} is the assimilation rate at reference temperature (µmol m^{-2} s^{-1}), $E_o(Ref._A)$ is the 'overall' activation energy of CO_2-assimilation (infinitesimally) close to the reference temperature (kJ mol^{-1}), and δ_A (kK^2) describes the dynamic change of $[E_o(Ref._A)]/\Re$, as measurement temperature increases.

With the 'Arrhenius-exponent' $[E_o(Ref._A)]/\Re$ (see Eqn. 1) defined as the temperature coefficient $\mu_{Ref.A}$ (in units of kK; Kruse *et al.* 2018), the three parameters defining the photosynthetic temperature response of an individual leaf can be determined from log_e-transformed expression of Eqn.1:

$$lnA = lnA_{ref} + \mu_{Ref.A} \times \left(\frac{T-T_{ref}}{T\times T_{ref}}\right) + \delta_A \times \left(\frac{T-T_{ref}}{T\times T_{ref}}\right)^2 \quad (2)$$

This article is protected by copyright. All rights reserved.

where $\ln A_{ref}$ is the $\log_e$- transformed rate of net photosynthesis at reference temperature (i.e., at 294K), $\mu_{Ref.A}$ denotes the slope of ln*A* at reference temperature and δ_A describes the dynamic change in $\mu_{Ref.A}$ as leaf temperature increases.

If we set x = $\left(\frac{T-T_{ref}}{T\times T_{ref}}\right)$, then the optimum temperature for *A* (T_{opt}), can be determined from the first derivative of Eqn.2 (i.e. *d*lnA/*d*x = 0):

$$x_{opt} = -\frac{1}{2}\frac{\mu_{Ref.A}}{\delta_A} \quad (3)$$

where $x_{opt} = \frac{T_{opt}-T_{ref}}{T_{opt}\times T_{ref}}$ $(1000/K)$, and δ_A is generally negative (for some notable exceptions, i.e. δ_A >0, see supporting information, Table S2). We expressed $T_{opt.}$ in units of °C. In order to test hypothesis 1, we compared T_{opt} with T_{growth}

Peak rates of photosynthesis (A_{opt}) were determined by insertion of x_{opt} into Eqn.2. We here define A_{opt} as the 'physiological capacity' of photosynthesis, i.e. the rate of CO_2-assimilation at light saturation and T_{opt}, recorded under ambient CO_2 ($c_a \approx$ 380-400 µmol mol^{-1}) and given stomatal conductance. A_{opt} differs from other measures of photosynthetic capacity like apparent V_{cmax} (carboxylation efficiency at low C_i), J_{max} (maximal electron transport capacity at saturating C_i and light, for RuBP- regeneration in the Calvin cycle), or light- saturated A_{max} at a set measurement temperature and saturating C_i (i.e., Aspinwall *et al.* 2016).

This article is protected by copyright. All rights reserved.

Accepted Article

We deliberately monitored temperature- dependent C_i at ambient CO_2, in order to test hypothesis 2 and 3. For this purpose, we extended the application of Eqn.2 to temperature-dependent stomatal conductance (G; mmol m^{-2} s^{-1}), and derived the three parameters $\ln G_{ref}$ (mmol m^{-2} s^{-1}), $\mu_{Ref.G}$ (kK) and δ_G (kK^2) (Table S2). This approach helps identify contrasting effects of growth temperature and irrigation on temperature sensitivities of net photosynthesis *versus* that of stomatal conductance (and thus the temperature sensitivity of C_i). In its logarithmic expression, water use efficiency ($WUE_i = A/G$) is defined as:

$$ln\left(\frac{A}{G}\right) = lnA - lnG \quad (4)$$

where A is given in µmol m^{-2} s^{-1} and G is given in mol m^{-2} s^{-1}. For the temperature sensitivity of WUE_i, it follows that:

$$ln\left(\frac{A}{G}\right) = \left(lnA_{ref} - lnG_{ref}\right) + (\mu_{Ref.A} - \mu_{Ref.G}) \times x + (\delta_A - \delta_G) \times x^2 \quad (5)$$

where $x = \frac{T - T_{ref}}{T \times T_{ref}}$ $(1000/K)$. From the first derivative of Eqn.5, we determined the temperature at which WUE is insensitive to small changes in measurement temperature (i.e., $d(\ln A - \ln G)/dx = 0$):

$$x_{equ.} = -\frac{1}{2}\frac{(\mu_{Ref.A} - \mu_{Ref.G})}{(\delta_A - \delta_G)} \quad (6)$$

where $x_{equ.} = \frac{T_{equ} - T_{ref}}{T_{equ} \times T_{ref}}$ $(1000/K)$. The 'equilibrium temperature' ($T_{equ.}$) is expressed in units of °C. At this temperature, C_i/C_a is insensitive to small changes in measurement temperature. To test for hypothesis 2, we compared T_{opt} with T_{equ}. We inserted x_{opt} into Eqn. 5, in order to determine WUE_i at T_{opt}, and to test for hypothesis 3.

This article is protected by copyright. All rights reserved.

Accepted Article

2.4. Sensitivity of stomatal conductance (*G*) towards net photosynthesis (*A*) versus vapour pressure deficit

Stomatal conductance depends on leaf temperature, as mediated through temperature-dependent *A* (Damour *et al.* 2010), but also varies with VPD that increases exponentially with cuvette air temperature. We used the approach outlined by Medlyn *et al.* (2011) to describe the sensitivity of *G* (mol m^{-2} s^{-1}) towards *A* relative to VPD:

$$G = g_o + 1.6 \times \left(1 + \frac{g_1}{D^{1-k}}\right) \times \frac{A}{c_a} \quad (7)$$

where g_o (mol m^{-2} s^{-1}) is the residual conductance when *A* (µmol m^{-2} s^{-1}) is zero, g_1 is related to the marginal water cost of carbon ($\lambda = \partial E/\partial A$), *k* is an empirical parameter that equals 0.5 when the response of *G* to *D* is optimal, C_a is the atmospheric [CO_2] (µmol mol^{-1}), and *D* is the vapour pressure deficit (kPa) (Medlyn *et al.* 2011, Duursma *et al.* 2014). We assumed that *k* =0.5 and plotted *G* derived from individual temperature response measurements against $A/\left(\sqrt{D} \times C_a\right)$. The slope of these plots (with n= 7, each) is dominated by g_1, but also varies with *D* (Eqn. 7; Medlyn *et al.* 2011), which cannot be neglected in the present study. Since the span of *D* was similar for all measurements (~1.5 kPa to ~6.5 kPa), we here denote the sensitivity of *G* towards $A/\left(\sqrt{D} \times c_a\right)$ as $1.6 \times g_1$*. R^2 of (significant) linear fits ranged between 0.3 – 0.99, and averaged 0.80 (median 0.85). Non-significant linear fits ($R^2 < 0.3$; $P > 0.05$), were not included in the further analysis

2.5. Statistical analysis

From a total of 240 available plants, 168 seedlings were randomly chosen for gas exchange measurements. With two failed measurements, 166 replicates were subjected to statistical analysis (Table S2). Data were subjected to analysis of variance (ANOVA), followed by

This article is protected by copyright. All rights reserved.

post-hoc Tukey HSD tests (STATISTICA, version 10.0, StatSoft, Inc, Tulsa, OK, USA), in order to evaluate the significance of season, irrigation treatment and day time on T_{opt}, A_{opt}, WUE_i at T_{opt}, R_{39}, (T_{opt}-T_{growth}) and (T_{equ}-T_{opt}), and to test hypothesis 1-3. For A_{opt} and WUE_i at T_{opt}, ANOVA was performed with $\log_e$-transformed data, to meet the criterion of homoscedasticity (Levene-test, STATISTICA).

We explored variation of temperature-dependent *A* and *G*, as defined by respective exponent parameters μ_{Ref} and δ, and compared results with the sensitivity of *G* towards VPD (relative to *A*). The exponent- parameters are mutually inter-dependent, and often highly correlated (Kruse *et al.* 2018). Factors that explain residual variation in this correlation were identified and quantified using General Linear Models. Effect sizes were estimated from partial η^2:

$$ {}_p\eta^2 = \frac{SS_{factor}}{SS_{factor} + SS_{residual}} \quad (8) $$

where ${}_p\eta^2$ indicates how much of the observed variation can statistically be explained by the factor under consideration (SS_{factor}).

3. Results

3.1. Leaf characteristics and plant growth

At the start of the experimental period (i.e., after T1), shoot biomass of well-watered seedlings averaged 27.8± 0.8 g fresh mass (average ±SE). It increased to 36.2± 2.1 g by the end of the experiment (after T4), irrespective of treatment season (Fig. S3). By the end of the experiment, shoot biomass of water-deprived plants averaged 31.2± 1.4 g in summer and winter. Thus, intermittent water shortage reduced shoot growth to ~40% of that achieved by

This article is protected by copyright. All rights reserved.

Accepted Article

fully watered plants. DM: FM- ratio of leaves increased from 0.43± 0.01 after T1 to 0.46± 0.01 after T4, but was hardly affected by treatment (Fig. S3). Leaf nitrogen contents were not significantly affected by season or irrigation treatment, and averaged at 15.1± 0.2 mg g^{-1} dry mass (Fig. S3). Leaf mass per area of pre-existing leaves was similar between treatments and averaged at 321± 10 g DM m^{-2}.

3.2. Instantaneous temperature responses of leaf gas exchange

Temperature responses of *A* and *G* (Fig. 3), were fitted to the extended Arrhenius- equation (see Fig. S4). Coefficients of determination (R^2) for Arrhenius-type fits ranged between 0.7-0.99, and averaged 0.95 for *A* (median 0.96), and averaged 0.93 for *G* (median 0.95).

Temperature responses of *A* and *G* were similar, but not the same. Consequently, *A*/*G* and C_i/C_a, which is inversely proportional to *A*/*G*, were not constant across measurement temperatures (Fig. 4). In summer, C_i/C_a decreased with decreasing slope as measurement temperature increased. In winter, by contrast, C_i/C_a increased with increasing slope as measurement temperature increased (Fig. 4e-h). The temperature at which C_i/C_a is most insensitive to changes in measurement temperature (i.e., where slopes of change become zero), is defined by the 'equilibrium temperature' (T_{equ}; Eqn. 6). It is apparent, and will be analyzed in greater detail below, that T_{equ} was located at warmer temperatures in summer- than in winter- acclimated leaves (Fig. 4e-h).

This article is protected by copyright. All rights reserved.

3.3. Photosynthetic acclimation: Shifts in T_{opt}

Season statistically explained 52% of the variation in T_{opt} (Fig. 5a-d, Table 1b), which averaged 27.4± 0.4°C in winter and 36.0± 0.6°C in summer. Another 18% of the variation was related to day time of measurements. On average, T_{opt} increased from 29.2± 0.6°C in the morning to 32.1± 0.7°C at midday, and further to 34.0± 0.9°C in the afternoon. Soil water deprivation (i.e., T2+T3 combined) had comparatively little effect on T_{opt} ($_p\eta^2$= 0.07, Table 1b), on average being ~2°C less than under well-watered conditions.

T_{opt} and T_{growth} were positively related (R^2: 0.53, P< 0.001; Fig. 6a). Overall, however, T_{opt} - $T_{growth} \neq 0$ (t-value: 6.3; P< 0.001), and T_{opt} was on average ~2.9°C greater than T_{growth} (28.8± 8.8°C; av.± SD). In particular, T_{opt} of winter-acclimated leaves was 6.1± 0.6°C (av.± SE) greater than T_{growth} (Fig. 7a). By contrast, for summer-acclimated leaves $T_{opt} \approx T_{growth}$. Similarly, T_{opt} was close to T_{growth} during severe drought, but 5.4± 1.2°C greater during recovery (Figs. 6a, 7b). T_{opt} hardly differed from T_{growth} at midday, but was significantly greater in the morning and afternoon (Fig. 7c). We conclude that variation in T_{opt} not only reflects acclimation to growth temperature. Departures of T_{opt} from T_{growth} seemingly depend on leaf water status (i.e., Ψ_l) at the time of measurement, as affected by long- term variation in soil water availability as well as seasonal and diurnal variation in VPD (and potential evapotranspiration).

This article is protected by copyright. All rights reserved.

Accepted Article

3.4. Photosynthetic acclimation: Shifts in A_{opt} and implications for WUE_i at T_{opt}

Season statistically explained 11% of the variation in lnA_{opt} (Table 1b). A_{opt} averaged 3.3± 0.2 μmol m^{-2} s^{-1} in winter and 5.5± 0.3 μmol m^{-2} s^{-1} in summer (Fig. 5e-h). Water deprivation affected A_{opt} more strongly than T_{opt} ($_p\eta^2$: 0.24; Table 1b). A_{opt} was reduced from 4.9± 0.2 μmol m^{-2} s^{-1} in fully watered plants to 3.0± 0.3 μmol m^{-2} s^{-1} during water deprivation (T2+T3). Reduction was particularly pronounced under severe drought (T3; Fig. 5g).

Under severe drought, A_{opt} was reduced more strongly than *G* (at T_{opt}), such that WUE_i at T_{opt} was significantly less than in fully watered plants (Fig. 5k) – in particular at midday and in the afternoon (Table 1b). That is, water- deprived plants generally operated at greater C_i than fully watered plants (Figs. 4f, g), and *A* was not limited by CO_2- supply *per se*. This contention was confirmed by independent measurement of bulk leaf $\delta^{13}C$- signatures, which averaged at -25.5± 0.1‰ in fully watered and -25.9± 0.1‰ in water- deprived plants (P= 0.02; Fig. S5).

We also measured leaf dark respiration at 39°C (i.e., R_{39}), in order to assess respiratory acclimation – that can affect both T_{opt} and A_{opt}. R_{39} averaged 2.4± 0.1 μmol m^{-2} s^{-1} in winter and 1.8± 0.1 μmol m^{-2} s^{-1} in summer (supplementary information Fig. S6, Table 1b). Reduction of R_{39} in summer was accompanied by shifts in T_{opt} to warmer temperature (on average +8.5°C) and greater A_{opt} (on average +2.2 μmol m^{-2} s^{-1}). Soil water deprivation added to seasonal reductions in R_{39}. In winter, R_{39} averaged 2.6± 0.1 μmol m^{-2} s^{-1} in fully watered plants and 2.2± 0.1 μmol m^{-2} s^{-1} under drought (T2+T3). In summer, R_{39} was reduced from 1.9± 0.1 μmol m^{-2} s^{-1} (full water) to 1.6± 0.1 μmol m^{-2} s^{-1} (drought). In contrast

This article is protected by copyright. All rights reserved.

to seasonal effects, however, drought- related reductions in R_{39} were accompanied by *reduced* A_{opt} (see first paragraph in this section). R_{39} averaged 2.6± 0.2 μmol m^{-2} s^{-1} in the morning, and was reduced to 2.0± 0.1 μmol m^{-2} s^{-1} at midday and 1.8± 0.1 μmol m^{-2} s^{-1} in the afternoon (Fig. S6, Table 1b). Concomitantly, T_{opt} increased on average by *c.* 4.5°C from morning to afternoon, while A_{opt} *decreased* by *c.* 1.4 μmol m^{-2} s^{-1}.

3.5. Coordination between temperature- dependent *A* and *G* for control of T_{equ} during acclimation

We hypothesized that during acclimation, A_{opt} would be recorded at that leaf temperature, where C_i is most insensitive to temperature variation – in order to allow for stable CO_2-supply and safe CO_2- assimilation at maximum rate under respective environmental conditions (i.e., $T_{equ} - T_{opt} = 0$). While T_{equ} and T_{opt} were strongly correlated (R^2: 0.70; Fig. 6b), $T_{equ} - T_{opt} \neq 0$ (t-value: 2.8; P= 0.005), and T_{equ} was on average ~0.8°C less than T_{opt} (31.7± 6.2°C; av.± SD). Strikingly, the effects of season, irrigation treatment and day time on the difference between T_{equ} and T_{opt} (Fig. 7d-f), were mostly inverse to those observed for the difference between T_{opt} and T_{growth} (Fig. 7a-e). We conclude that photosynthetic acclimation associated with shifts in T_{opt} and A_{opt}, reflects a trade- off between maximization of *A* and the risk of imbalances in CO_2-supply to chloroplasts.

3.6. Similarities and differences between temperature sensitivities of *A* and *G*

Temperature sensitivities of *A* and *G* were analyzed in greater detail, in order to elucidate acclimation-induced shifts in T_{opt} and T_{equ}. There was considerable variation in exponent parameters, which define respective temperature sensitivities and are mutually inter-

This article is protected by copyright. All rights reserved.

Accepted Article

dependent (Fig. 8). Residual variation in the correlation between μ_{Ref} and δ was related to treatment conditions, in particular season (Fig. 8). We used General Linear Models with a mixture of predictor continuous variables to identify and quantify sources of residual variation (supplementary information Table S3). For both *A* and *G*, three variables captured most of the variation in δ- parameter. First, δ- parameter was tightly related to μ_{Ref} ($_p\eta^2$: 0.83-0.88; supplementary information, Fig. S7). Secondly, δ_A and δ_G exhibited similar dependency on T_{opt} ($_p\eta^2$: 0.56-0.62; Fig. S7). However, δ_A was more sensitive to lnA_{opt} than lnA_{ref}, whereas δ_G was more sensitive to lnG_{ref} than lnG_{opt} (Table S3). δ_A and δ_G showed contrasting dependency on photosynthetic capacity at optimum temperature and stomatal aperture at reference temperature, respectively. δ_A varied positively by *c.* 20 kK^2 over the range of recorded lnA_{opt}, if other factors are constant (Fig. S7c). While δ_G also varied by *c.* 23 kK^2 over the range of recorded ln$G_{ref,}$ this relation was negative (Fig. S7f).

3.7. Sensitivity of stomatal conductance towards leaf temperature and vapor pressure deficit (VPD)

Most conspicuously, water deprivation during T2+T3 significantly reduced the temperature sensitivity of stomatal conductance (i.e., $\mu_{Ref.G}$ and δ_G), while conductance at low reference temperature (i.e., lnG_{ref}) was hardly affected (Table 2). Hence, stomatal conductance also showed reduced sensitivity to VPD during drought (Figs. 9b, c). As a result, leaf transpiration was significantly reduced at greater VPD (Figs. 9f, g). This analysis does not tell much about the control of *G*, which depends on both temperature-dependent *A* and VPD. For example, stomatal conductance of water-deprived plants was significantly reduced at T_{opt} ($_p\eta^2$: 0.18; effect on lnG_{opt} not shown in Table 2), but lnA_{opt} was reduced even stronger ($_p\eta^2$: 0.23, Table 2; also see above section 3.4). Data obtained for *G* during T2+T3 were plotted against

This article is protected by copyright. All rights reserved.

Accepted Article

$A/(\sqrt{D} \times c_a)$ (supplementary information, Fig. S8), in order to analyze sensitivity of *G* towards *A* relative to VPD (Eqn. 7), and we derived the following linear regression equations:

$$G = 0.016 \text{ mol m}^{-2}\text{s}^{-1} + 1.8 \times \frac{A}{\sqrt{D} \times c_a} \qquad \text{(winter, +H}_2\text{O)}$$

$$G = 0.011 \text{ mol m}^{-2}\text{s}^{-1} + 3.0 \times \frac{A}{\sqrt{D} \times c_a} \qquad \text{(winter, -H}_2\text{O)}$$

$$G = 0.005 \text{ mol m}^{-2}\text{s}^{-1} + 5.5 \times \frac{A}{\sqrt{D} \times c_a} \qquad \text{(summer, +H}_2\text{O)}$$

$$G = 0.008 \text{ mol m}^{-2}\text{s}^{-1} + 5.0 \times \frac{A}{\sqrt{D} \times c_a} \qquad \text{(summer, -H}_2\text{O)}$$

where the intercept is equivalent to residual conductance g_o, and the slope is defined as $1.6 \times g_1^*$. Seasonal differences in g_o and g_1^* were more pronounced than effects of irrigation treatment (also see Fig. S9). Stomatal conductance was more sensitive to *A* relative to *D* in summer than in winter (greater g_1^* in summer), but drought effects on g_1^* varied between season.

4. Discussion

As poikilothermic organisms, plants have to cope with potentially large variation in leaf temperature, which strongly influences rates of biochemical reactions - including those that drive photosynthesis. Selection pressures to optimize photosynthesis under given climatic conditions required evolutionary solutions to either constrain leaf temperature (Helliker & Richter 2008), or to allow for physiological acclimation if leaf temperature should vary. Both of these control mechanisms are realized in plants (Yamori *et al* 2014, Wright *et al.* 2017). Species adapted to hot and semi-arid environments, for example, have comparatively small leaves (i.e, as compared to wet- tropical species), favoring convective over latent heat dissipation (greater Bowen-ratio; Wright *et al.* 2017). As to physiological acclimation in date

This article is protected by copyright. All rights reserved.

Accepted Article

palm, we hypothesized that optimal leaf temperature for photosynthesis (T_{opt}) would track changes in ambient growth temperature (T_{growth}).

4.1. Acclimatory shifts in T_{opt}

Although T_{opt} was recorded under different micro-meteorological conditions than those prevailing in our growth chambers, we found clear evidence for thermal acclimation of T_{opt}. About ~50% of the variation in T_{opt} was related to variation in T_{growth} (Fig. 6a), underpinning strong diurnal and, in particular, seasonal effects on T_{opt} (Fig. 5a-d, Table 1b). T_{opt} of date palm varied between 20- 45°C, as has also been observed in a meta-analysis of data reported for various C_3-species (Yamori *et al.* 2014). Deviation from a 1: 1- line between T_{opt} and T_{growth} in our study (Fig. 6a), was also strikingly similar to published data (Fig. 5a in Yamori *et al.* 2014). For remaining differences between T_{opt} and T_{growth} (i.e., $T_{opt} - T_{growth} \neq 0$), we consider two sources of additional variation. First, T_{growth} does not necessarily reflect leaf temperature under respective growth conditions, owing to variation in latent heat dissipation. Our results suggest that transpiration played a proportionally greater role in leaf cooling during summer as compared to winter, at least for fully watered plants (Fig. 9e-h). Secondly, the temperature optimum of *A* not only acclimates to leaf temperature (under growth conditions), but seems also responsive to leaf water status at the time of measurement. Leaf water potential declines over time, if water uptake and transport cannot keep pace with transpiration - frequently observed under high VPD (and T_{growth}), or low soil water availability. Reduced Ψ_l most likely accounts for observations that T_{opt} was closer to T_{growth} in summer, at midday or during drought (Fig. 7a-c). Complex interdependencies between incident radiation, T_{growth}, VPD, transpiration, leaf water potential and –temperature (i.e., O'Sullivan *et al.* 2017), could also explain observations that T_{opt} tracked T_{growth} under some

This article is protected by copyright. All rights reserved.

Accepted Article

circumstances (Battaglia *et al.* 1996, Gunderson *et al.* 2010, Way & Oren 2010, Slot & Winter 2017), whereas thermal acclimation of T_{opt} was not evident in other studies (Warren 2008, Dillaway & Kruger 2010, Drake *et al.* 2016, Kruse *et al.* 2017b)

4.2. Physiological mechanisms driving thermal acclimation of T_{opt}

Our understanding of biochemical/physiological mechanisms that contribute to thermal acclimation of T_{opt}, has been significantly advanced in previous decades (reviewed by Hikosaka *et al.* 2006, Sage & Kubien 2007, Lin *et al.* 2012, Yamori *et al.* 2014). Biochemical acclimation affects a plethora of components that comprise the 'photosynthetic machinery'. Most consistently among C_3- species, heat exposure triggers expression of a heat-stable Rubisco- activase or re- adjustment of electron transport capacity (Salvucci & Crafts-Brandner 2004, Schrader *et al.* 2004, Sage & Kubien 2007), or both. Such biochemical acclimation to longer- term, seasonal shifts in T_{growth} helps maintain the balance between RuBP – carboxylation and - regeneration capacities (*sensu* Medlyn *et al.* 2002). Diffusion velocity of thylakoid electron carriers, for example, is strongly temperature- dependent, but can physiologically be controlled via adjustment of membrane viscosity (Barber *et al.* 1984, Ott *et al.* 1999). This may entail alterations in membrane lipid composition (Raison *et al.* 1980, Safronov *et al.* 2017), or membrane protein abundances (Onoda *et al.* 2005, Zhu *et al.* 2007) - such that temperature sensitivity of (lateral) thylakoid electron transport can match stromal processes.

This article is protected by copyright. All rights reserved.

Stabilization of membrane functioning may also be accomplished by isoprene production (Sharkey 2005). We recently observed increased capacity of isoprene emission in heat-acclimated date palm leaves (Arab *et al.* 2017). Temperature-dependent isoprene emission (Monson *et al.* 2012, Arab *et al.* 2017), could also account for some short-term, diurnal variation in T_{opt}.

Thermal acclimation changes the temperature sensitivity of biochemical capacities, becoming apparent in altered V_{cmax} and/or J_{max} at standard reference temperature (usually 25°C; Atkin *et al.* 2015, Lin *et al.* 2013, Crous *et al.* 2018), or altered activation energy close to T_{ref} (Hikosaka *et al.* 2006, Kositsup *et al.* 2009), or shifts in T_{opt} of V_{cmax} and/or J_{max} (Kattge & Knorr 2007, Yamori *et al.* 2008, Vårhammer *et al.* 2015). A recent meta-analysis using a peaked Arrhenius- type function to describe the temperature dependency of V_{cmax} and J_{max}, identified parameters that acclimate to T_{growth} and – positively or negatively - correlate with T_{opt} of *A* at ambient CO_2 (see Kumarathunge *et al.* 2019). Biochemical acclimation undoubtedly facilitates shifts in T_{opt} of *A* (Kumarathunge *et al.* 2019), although it will still remain difficult to attribute shifts in specific, rate-limiting processes to the position of T_{opt} (Yamori *et al.* 2014; further discussed in Section 4.5.).

Also respiratory acclimation is thought to account for shifts in T_{opt} (and A_{opt}) (Lin *et al.* 2012, Way & Yamori 2014). This is particularly important for species with slow rates of leaf net photosynthesis such like spruce (Way & Sage 2008), or date palm. While respiratory acclimation is better described by respiratory responses over a range of measurement temperatures (instead of point measurements at 39°C, Kruse *et al.* 2011), and respiration is generally less in the light than in the dark (Tcherkez *et al.* 2017), we observed significant

This article is protected by copyright. All rights reserved.

Accepted Article

reductions in R_{39} at greater T_{growth} indicating thermal acclimation of leaf respiration (i.e., Atkin *et al.* 2015, Reich *et al.* 2016). Drought added to thermally- induced reductions in R_{39}, similar to observations made for *Eucalyptus saligna* (Crous *et al.* 2011).

4.3. Do imbalances in CO_2- supply to chloroplasts trigger acclimation to altered environmental conditions?

The central novel finding of our study was the close relationship between T_{opt} and T_{equ} (Fig. 6b), essentially confirming hypothesis 2 and suggesting tight coordination between *A* and *G* for stabilization of CO_2 – supply to chloroplasts, irrespective of changes in T_{growth} and water availability. In particular, thermal acclimation altered the sensitivity of stomata towards *A* relative to VPD. This sensitivity is notoriously variable (Miner *et al.* 2017), but our results corroborate earlier reports that acclimation to warm temperatures increases g_1^* (Leuning 1990, Medlyn *et al.* 2011), commensurate with concomitant shifts in T_{equ} (and T_{opt}; Lin *et al.* 2012, Duursma 2014). Our results also accord with observations that drought alone has little effect on g_1^* in species adapted to xeric sites (Héroult *et al.* 2013).

To some degree, imbalances in chloroplast CO_2-concentration (C_c) can be buffered by quick adjustments in mesophyll conductance to CO_2- transfer (G_m; Flexas *et al.* 2012). G_m differs between species (von Caemmerer & Evans 2015), and often increases exponentially with measurement temperature – suggesting that G_m is under enzymatic control (Flexas *et al.* 2012). While C_i varies over a broader range of measurement temperatures (i.e., further removed from T_{equ}; Fig. 4e-h), C_c has been shown to remain surprisingly constant (Warren & Dreyer 2006, Warren 2008). There is also some evidence for longer- term acclimation of G_m to T_{growth} (Yamori *et al.* 2006), possibly before acclimatory effects on V_{cmax} or J_{max} become apparent, as in boreal and temperate tree species (Dillaway & Kruger 2010).

This article is protected by copyright. All rights reserved.

We propose that plants 'sense' major imbalances in C_c that could result in (harmful) ROS generation and trigger acclimation. Acclimation of leaf gas exchange might thus be viewed as a process to restore the balance between CO_2- supply and – demand. Recovery from drought, for example, swiftly re-established physiological capacity of photosynthesis (A_{opt}; Figs. 3d, 5h), albeit associated with reduced 'safety margins' (i.e., $T_{equ} - T_{opt} < 0$; Fig. 7e).

4.4. Acclimation to drought: Date palms play it safe

Flexas & Medrano (2002) highlighted bi-phasic responses of C_i to drought in many species. Stomatal closure usually first reduces C_i. With progressing drought, processes like carboxylation efficiency are increasingly impaired (Parry *et al.* 2002, Xu & Baldocchi 2003, Chaves *et al.* 2009), counter-acting reductions in C_i. Biochemical limitations of *A* under mild drought are generally reversible upon restoration of soil water availability. However, extended drought may cause *G* to drop below ~50 mmol m^{-2} s^{-1}, associated with an increase of C_i (Brodribb 1996, Flexas & Medrano 2002).

In date palm, even mild drought had an immediate effect on A_{opt} (Fig. 5f), which was generally reduced more strongly than G_{opt} during water- deprivation. As a result, water-deprived plants operated at greater C_i than fully watered plants (Figs. 4f, g). This unusual result was confirmed by a slight, but significant increase of $\delta^{13}C_l$ under drought. In many other C_3-species, drought triggers a decline of $\delta^{13}C_l$ (Farquahr *et al.* 1989, Ehleringer *et al.* 1992). Nonetheless, the extent of drought effects on $\delta^{13}C_l$ varies between species, and even between genotypes of the same species (Donavan & Ehleringer 1994, Pita *et al.* 2001, Cernusak *et al.* 2013).

This article is protected by copyright. All rights reserved.

Accepted Article

Phoenix dactylifera is a slow-growing species with robust, sclerophyllous leaves (i.e., comparatively large LMA, low leaf-N contents and low A_{opt}). Even with full water supply, stomatal conductance of date palms is less than considered symptomatic of severe water-stress in other species (G_{opt} < 50 mmol m^{-2} s^{-1}, Fig. 3e-h; see Medrano *et al.* 2002). These physiological traits reflect adaptation to a xeric environment, where slow growth and conservative water use are evolutionarily advantageous strategies (Mäkela *et al.* 1996). Drought quickly arrested growth in date palm, and declining demand for anabolic products seemingly caused down-regulation of A_{opt}, as has also been observed, albeit less quickly, for other measures of photosynthetic capacity in different species (i.e., V_{cmax}; Parry *et al.* 2002, Joseph *et al.* 2014). Swift, over- proportional reduction of A_{opt} in water- deprived date palm facilitated photosynthesis at slow, but safe rates.

4.5. Outlook: The significance of δ- parameter

Elucidating the nature of δ- parameter seems a promising avenue to improved mechanistic understanding of *in vivo* flux control. Previous findings that instantaneous temperature responses of leaf net photosynthesis and dark respiration (*R*) can be described by the same, extended Arrhenius- equation (Kruse *et al.* 2017b), imply some common features in the regulation of both *A* and *R*.

As noted above (Section 4.2.), Calvin- cycle activity is controlled in myriad ways, most notably encompassing the thioredoxin system (Buchanan & Balmer 2005) and Rubisco-activase activity – itself dependent on ATP/ADP and NADPH/NADP (Portis 2003). We previously argued that constant temperature- dependency of 'overall' activation energy is an

This article is protected by copyright. All rights reserved.

Accepted Article

emergent property of metabolic networks such like the Calvin- cycle (Kruse *et al.* 2017a). Monotonous change of overall activation energy across measurement temperatures, even extending beyond T_{opt}, suggests tight coordination between the component processes. It has also been shown that rates of CO_2- assimilation correlate with those of thylakoid electron transport (i.e., Niinemets *et al.* 1999, Aspinwall *et al.* 2016, Kruse *et al.* 2017a), and that declining rates above T_{opt} are generally reversible (if measurement temperatures had not exceeded *c.* 40-45°C and produced irreversible damage; June *et al.* 2004).

We proposed that δ_A ultimately reflects proportions of cyclic *versus* non- cyclic electron flow, as controlled by cellular demand for ATP *versus* NADPH (Kruse *et al.* 2017a). For example, 'speed' of ATP- turnover *relative to* NADPH- turnover depends on reduction state of anabolic products (sucrose, starch, amino acids, fatty acids, etc.) and many other cellular functions (i.e., ATP- demand for protein turnover or maintenance of membrane potentials, etc.) - affecting the shape of photosynthetic temperature responses (that is, δ_A). Peak rates of *A* (that is, A_{opt}) heavily depend on demand for anabolic products destined for export (i.e., sucrose, amino acids), and, by extension, on plant growth (Körner 2013). Reduced rates of A_{opt} (and R_{39}) under drought likely reflect reduced demand for energy and reducing power (ATP + NADPH), for synthesis and export of photosynthate (Atkin & Macherel 2009). Temperature sensitivity of stomatal conductance, on the other hand, seems primarily controlled to ensure stable CO_2- supply to chloroplasts (Section 4.3.).

Summarily, date palm exhibits remarkable capability to coordinate acclimation in leaf- level T_{opt}, A_{opt} and T_{equ}, with whole plant growth, which we regard as 'optimal' under environmental conditions to which this species is adapted. We expect that plant species adapted to different climates will exhibit alternative acclimation strategies.

This article is protected by copyright. All rights reserved.

Accepted Article

Accepted Article

Acknowledgements

This study was financially supported by the King Saud University, Saudi-Arabia, and the University of Sydney, Australia. We thank the technical team at the Helmholtz center, München, for tending the plants and the technical infrastructure. We thank Prof. Medlyn and four anonymous reviewers for many helpful comments on earlier draft(s) of this manuscript.

Author contributions

SA, RH and HR conceived and managed the project. JöK, BW, AG, JüK and J-P S designed the experiment. BW, AG and J-P S ensured excellent simulation of Saudi-Arabian climate. JöK performed physiological measurements and analyzed the data. JöK, MA and HR led interpretation of the results. Every author contributed to writing the manuscript.

References

Aphalo PJ, Jarvis PG. 1991. Do stomata respond to relative humidity? *Plant, Cell and Environment* **14**: 127-132.

Arab L, Kreuzwieser J, Kruse J, Zimmer I, Ache P, Alfarraj S, Al-Rasheid KAS, Schnitzler J-P, Hedrich R, Rennenberg H. 2016. Acclimation to heat and drought – lessons to learn from the date palm (*Phoenix dactylifera*). *Environmental and Experimental Botany* **125**: 20-30.

Aspinwall MJ, Drake JE, Company C, Vårhammer A, Ghannoum O, Tissue DT, Reich PB, Tjoelker MG. 2016. Convergent acclimation of leaf photosynthesis and respiration to prevailing ambient temperatures under current and warmer climates in *Eucalyptus tereticornis*. *New Phytologist* **212**: 354-367.

Assmann SM. 1999. The cellular basis of guard cell sensing of rising CO_2. *Plant, Cell and Environment* **22:** 629-637.

Atkin OK, Macherel D. 2009. The crucial role of plant mitochondria in orchestrating drought tolerance. *Annals of Botany* **103**: 581-597.

Atkin OK, Bloomfield KJ, Reich PB, Tjoelker MG, Asner GP, Bonal D *et al*. 2015. Global variability in leaf respiration in relation to climate, plant functional types and leaf traits. *New Phytologist* **206**: 614-636.

This article is protected by copyright. All rights reserved.

Ball JT, Woodrow IE, Berry JA. 1987. A model predicting stomatal conductance and its contribution to the control of photosynthesis under different environmental conditions. Progress in Photosynthesis Research (ed. I. Biggins), pp. 221-224. Martinus Nijhoff Publishers, Netherlands.

Barber J, Ford RC, Mitchell RAC, Millner PA. 1984. Chloroplast thylakoid fluidity and its sensitivity to temperature. *Planta* **161**: 948-954.

Battaglia M, Beadle C, Loughhead S. 1996. Photosynthetic temperature responses of *Eucalyptus globulus* and *Eucalyptus nitens*. *Tree Physiology* **16**: 81-89.

Berry JA, Björkman O. 1980. Photosynthetic response and adaptation to temperature in higher plants. *Annual Review of Plant Physiology* **31**: 491-543.

Boyer JS. 1976. Photosynthesis at low water potentials. *Philosophical Transactions of the Royal Society*, Series B, **273**: 501-512.

Brodribb T. 1996. Dynamics of changing intercellular CO_2 concentration (c_i) during drought and determination of minimum functional c_i. *Plant Physiology* **111**: 179-185.

Buchanan BB, Balmer. 2005. Redox regulation: A broadening horizon. *Annual Reviews in Plant Biology* **56**: 187-220.

von Caemmerer S, Evans JR. 2015. Temperature responses of mesophyll conductance differ greatly between species. *Plant, Cell & Environment* **38**: 629-637.

Cernusak LA, Ubierna N, Winter K, Holtum JAM, Marshall JD, Farquhar GD. 2013. Environmental and physiological determinants of carbon isotope discrimination in terrestrial plants. *New Phytologist* **200**: 950-965.

Chaves MM, Flexas J & Pinheiro C. 2009. Photosynthesis under drought and salt stress: regulation mechanisms from whole plant to cell. *Annals of Botany* **103**: 551-560.

Cornic G. 2000. Drought stress inhibits photosynthesis by decreasing stomatal aperture – not by affecting ATP synthesis. *Trends in Plant Science* **5**: 187-188.

Cowan IR. 1977. Stomatal behavior and environment. *Advances in Botanical Research* **4**: 117-288.

Cowan IR, Farquhar G. 1977. Stomatal function in relation to leaf metabolism and environment. In: *Integration of Activity in the Higher Plant* (ed. Jennings DH), pp. 471-505. Cambridge University Press, Cambridge.

Crous KY, Zaragoza- Castells J, Löw M, Ellsworth DS, Tissue DT, Tjoelker MG, Barton CVM, Gimeno TE, Atkin OK. 2011. Seasonal acclimation of leaf respiration in *Eucalyptus saligna* trees: impacts of elevated atmospheric CO_2 and summer drought. *Global Change Biology* **17**: 1560-1576.

This article is protected by copyright. All rights reserved.

Crous KY, Drake JE, Aspinwall MJ, Sharwood RE, Tjoelker MG, Ghannoum O. 2018. Photosynthetic capacity and leaf nitrogen decline along a controlled climate gradient in provenances of two widely distributed *Eucalyptus* species. *Global Change Biology* **24**: 4626-4644.

Damour G, Vandame M, Urban L. 2009. Long-term drought results in a reversible decline in photosynthetic capacity in mango leaves, not just a decrease in stomatal conductance. *Tree Physiology* **29**: 675-684.

Damour G, Simonneau T, Cochard H, Urban L. 2010. An overview of models of stomatal conductance at the leaf level. *Plant, Cell and Environment* **33**: 1419-1438.

Dillaway D, Kruger EL. 2010. Thermal acclimation of photosynthesis: a comparison of boreal and temperate tree species along a latitudinal transect. *Plant, Cell and Environment* **33**: 888-899.

Donovan LA, Ehleringer. 1994. Potential for selection on plants for water-use efficiency as estimated by carbon isotope discrimination. *American Journal of Botany* **81**: 927-935.

Drake JE, Tjoelker MG, Aspinwall MJ, Reich PB, Barton CVM, Medlyn BE, Duursma RA. 2016. Does physiological acclimation to climate warming stabilize the ratio of canopy respiration to photosynthesis? *New Phytologist* **211**: 850-863.

Duursma RA, Barton CVM, Lin Y-S, Medlyn BE, Eamus D, Tissue DT, Ellsworth DS, McMurtrie RE. 2014. The peaked response of transpiration to vapour pressure deficit in field conditions can be explained by the temperature optimum of photosynthesis. *Agricultural and Forest Meteorology* **189-190**: 2-10.

Eamus D, Taylor DT, Macinnis-Ng CMO, Shanahan S, de Silva L. 2008. Comparing model predictions and experimental data for the response of stomatal conductance and guard cell turgor to manipulations of cuticular conductance, leaf-to-air vapour pressure difference and temperature: feedback mechanisms are able to account for all observations. *Plant, Cell and Environment* **31**: 269-277.

Ehleringer JR, Phillips SL & Comstock JP. 1992. Seasonal variation in the carbon isotopic composition of desert plants. *Functional Ecology* **6**: 396-404.

Farquhar GD, Ehleringer JR, Hubick KT. 1989. Carbon isotope discrimination and photosynthesis. *Annual Review of Plant Physiology and Plant Molecular Biology* **40**: 503-537.

Farquhar GD, Sharkey TD. 1982. Stomatal conductance and photosynthesis. *Annual Review of Plant Physiology* **33**: 317-345.

Flexas J, Medrano. 2002. Drought-inhibition of photosynthesis in C_3 plants: Stomatal and non-stomatal limitations revisited. *Annals of Botany* **89**: 183-189.

This article is protected by copyright. All rights reserved.

Flexas J, Barón M, Bota J, Ducruet J-M, Gallé A, Galmés J, Jiménez M, Pou A, Ribas-Carbó M, Sajnani C,Tomàs M, Medrano H. 2009. Photosynthesis limitations during water stress acclimation and recovery in the drought-adapted *Vitis* hybrid Richter-110 (*V.berlandieri* × *V.rupestris*). *Journal of Experimental Botany* **60**: 2361-2377.

Flexas J, Barbour MM, Brendel O, Cabrera HM, Carriquí M, Díaz-Espejo A, Douthe C, Dreyer E, Ferrio JP, Gago J, Gallé A, Galmés J, Kodama N, Medrano H, Niinemets Ü, Peguero-Pina JJ, Pou A, Ribas-Carbó M, Tomás M, Tosens T, Warren CR. 2012. Mesophyll diffusion conductance to CO_2: An unappreciated central player in photosynthesis. *Plant Science* **193**: 70-84.

Gunderson CA, O'Hara KH, Campion CM, Walker AW, Edwards NT. 2010. Thermal plasticity of photosynthesis: the role of acclimation in forest responses to a warming climate. *Global Change Biology* **16**: 2272-2286.

Helliker BR, Richter SL. 2008. Subtropical to boreal convergence of tree-leaf temperatures. *Nature* **454**: 511-514.

Héroult A, Lin Y-S, Bourne A, Medlyn BE, Ellsworth DS. 2013. Optimal stomatal conductance to photosynthesis in climatically contrasting *Eucalyptus* species under drought. *Plant, Cell and Environment* **36**: 262-274.

Hikosaka K, Ishikawa K, Borjigidai A, Onoda Y. 2006. Temperature acclimation of photosynthesis: mechanisms involved in the changes in temperature dependence of photosynthetic rate. *Journal of Experimental Botany* **57**: 291-302.

Joseph T, Whitehead D, Turnbull MH. 2014. Soil water availability influences the temperature response of photosynthesis and respiration in a grass and woody shrub. *Functional Plant Biology* **41**: 468-481.

June T, Evans JR, Farquhar GD. 2004. A simple new equation for the reversible temperature dependence of photosynthetic electron transport: a study on soybean leaf. *Functional Plant Biology* **31**: 275–283.

Kattge J, Knorr W. 2007. Temperature acclimation in a biochemical model of photosynthesis: a reanalysis of data from 36 species. *Plant, Cell and Environment* **30**: 1176-1190.

Körner C. 2013. Growth controls photosynthesis – mostly. *Nova Acta Leopoldina* **114**: 273-283.

Kositsup B, Montpied P, Kasempsad P, Thaler P, Améglio T, Dreyer E. 2009. Photosynthetic capacity and temperature responses of photosynthesis of rubber tree (*Hevea brasiliensis* Müll. Arg.) acclimate to changes in ambient temperatures. *Trees – Structure and Function* **23**: 357-365.

Kruse J, Rennenberg H, Adams MA. 2011. Steps towards a mechanistic understanding of respiratory temperature responses. *New Phytologist* **189**: 659-677.

This article is protected by copyright. All rights reserved.

Accepted Article

Kruse J, Turnbull T, Adams MA. 2012. Disentangling respiratory acclimation and adaptation to growth temperature by *Eucalyptus* spp. *New Phytologist* **195**: 149-163.

Kruse J, Hopman P, Rennenberg H, Adams MA. 2012. Modern tools to tackle traditional concerns: Evaluation of site productivity and *Pinus radiata* management via $\delta^{13}C$ and $\delta^{18}O$-analysis of tree-rings. *Forest Ecology and Management* **285**: 227-238.

Kruse J, Alfarraj S, Rennenberg H, Adams MA. 2017a. A novel mechanistic interpretation of instantaneous temperature responses of leaf net photosynthesis. *Photosynthesis Research* **129**: 43-58.

Kruse J, Adams MA, Kadinov G, Arab L, Kreuzwieser J, Schulze W, Rennenberg H. 2017b. Characterization of photosynthetic acclimation in *Phoenix dactylifera* by a modified Arrhenius equation originally developed for leaf respiration. *Trees – Structure and Function* **31**: 623-644.

Kruse J, Rennenberg H, Adams MA. 2018. Three physiological parameters capture variation in leaf respiration of *Eucalyptus grandis*, as elicited by short-term changes in ambient temperature, and differing nitrogen supply. *Plant, Cell & Environment* **41**: 1369-1382.

Kumarathunge DP, Medlyn BE, Drake JE, Tjoelker MG, Aspinwall MJ, Battaglia M, Cano FJ, Carter KR, Cavaleri MA, Cernusak LA, Chambers JQ, Crous KY, De Kauwe MG, Dillaway DN, Dreyer E, Ellsworth DS, Ghannoum O, Han Q, Hikosaka K, Jensen AM, Kelly JWG, Kruger EL, Mercado LM, Onoda Y, Reich PB, Rogers A, Slot M, Smith NG, Tarvainen L, Tissue DT, Togashi HF, Tribuzy ES, Uddling J, Vårhammer A, Wallin G, Warren JM, Way D. 2019. Acclimation and adaptation components of the temperature dependence of plant photosynthesis at the global scale. *New Phytologist* **222**: 768-784.

Lawlor DW. 2002. Limitation to photosynthesis in water-stressed leaves: Stomata *vs.* Metabolism and the role of ATP. *Annals of Botany* **89**: 871-885.

Lawlor DW, Cornic G. 2002. Photosynthetic carbon assimilation and associated metabolism in relation to water deficits in higher plants. *Plant, Cell & Environment* **25**: 275- 294.

Lawlor DW, Tezara W. 2009. Causes of decreased photosynthetic rate and metabolic capacity in water-deficient leaf cells: a critical evaluation of mechanisms and integration of processes. *Annals of Botany* **103**: 561-579.

Leuning R. 1990. Modelling stomatal behavior and photosynthesis of *Eucalyptus grandis*. *Australian Journal of Plant Physiology* **17**: 159-175.

Leuning R. 1995. A critical appraisal of a combined stomatal-photosynthesis model for C_3 plants. *Plant, Cell and Environment* **18**: 339-355.

Lin Y-S, Medlyn BE, Ellsworth DS. 2012. Temperature responses of leaf net photosynthesis: the role of component processes. *Tree Physiology* **23**: 219-231.

This article is protected by copyright. All rights reserved.

Accepted Article

Lin Y-S, Medlyn BE, De Kauwe MG, Ellsworth DS. 2013. Biochemical photosynthetic responses to temperature: how do interspecific differences compare with seasonal shifts? *Tree Physiology* **33**: 793-806.

Macfarlane C, White DA, Adams MA. 2004. The apparent feed-forward response to vapor pressure deficit of stomata in droughted, field-grown *Eucalyptus globulus* Labill. *Plant, Cell & Environment* **27**: 1268-1280.

Mäkelä A, Berninger F, Hari P. 1996. Optimal control of gas exchange during drought: Theoretical analysis. *Annals of Botany* **77**: 461-467.

Medlyn BE, Dreyer E, Ellsworth D, Harley PC, Kirschbaum MUF, Le Roux X, Montpied P, Strassmeyer J, Walcroft A, Wang K, Loustau D. 2002. Temperature response of parameters of a biochemically based model of photosynthesis. II. A review of experimental data. *Plant, Cell & Environment* **25**: 1167-1179.

Medlyn BE, Duursma RA, Eamus D, Ellsworth DS, Prentice IC, Barton CVM, Crous KY, De Angelis P, Freeman M, Wingate L. 2011. Reconciling the optimal and empirical approaches to modelling stomatal conductance. *Global Change Biology* **17**: 2134-2144.

Medrano H, Escalona JM, Bota J, Gulias J, Flexas J. 2002. Regulation of photosynthesis of C_3 plants in response to progressive drought: Stomatal conductance as a reference parameter. *Annals of Botany* **89**: 895-905.

Miner GL, Bauerle WL, Baldocchi DD. 2017. Estimating the sensitivity of stomatal conductance to photosynthesis: a review. *Plant, Cell and Environment* **40**: 1214-1238.

Monson RK, Grote R, Niinemets Ü, Schnitzler J-P. 2012. Modeling the isoprene emission rate from leaves. *New Phytologist* **195**: 541-559.

Mott KA. 1988. Do stomata respond to CO_2 concentrations other than intercellular? *Plant Physiology* **86**: 200-203.

Mott KA, Parkhurst DF. 1991. Stomatal responses to humidity in air and helox. *Plant, Cell and Environment* **14**: 509-515.

Niinemets Ü, Oja V, Kull O. 1999. Shape of leaf photosynthetic electron transport versus temperature response curve is not constant along canopy light gradients in temperate deciduous trees. *Plant, Cell and Environment* **22**: 1497-1514.

Onoda Y, Hikosaka K, Hirose T. 2005. The balance between RuBP carboxylation and RuBP regeneration: a mechanism underlying the interspecific variation in acclimation of photosynthesis to seasonal changes in temperature. *Functional Plant Biology* **32**: 903-910.

O'Sullivan O, Heskel MA, Reich PB, Tjoelker MG, Weerasinghe LK, Penillard A, Zhu L, Egerton JJG, Bloomfield KJ, Creek D, Bahar NHA, Griffin KL, Hurry V, Meir P, Turnbull MH, Atkin OK. 2017. Thermal limits of leaf metabolism across biomes. *Global Change Biology* **23**: 209-223.

This article is protected by copyright. All rights reserved.

Accepted Article

Oren R, Sperry JS, Katul GG, Pataki DE, Ewers BE, Phillips N, Schäfer KVR. 1999. Survey and synthesis of intra- and interspecific variation in stomatal sensitivity to vapor pressure deficit. *Plant, Cell and Environment* **22**: 1515-1526.

Ott T, Clarke J, Birks K, Johnson G. 1999. Regulation of the electron transport chain. *Planta* **209**: 250-258.

Parry MAJ, Andralojc PJ, Khan S, Lea PJ, Keys AJ. 2002. Rubisco activity: Effects of drought stress. *Annals of Botany* **89**: 833-839.

Pita P, Soria F, Canas I, Toval G, Pardos JA. 2001. Carbon isotope discrimination and its relationship to drought under field conditions in genotypes of *Eucalyptus globulus*. *Forest Ecology and Management* **141**: 211-221.

Portis AR Jr. 2003. Rubisco Activase: Rubisco's catalytic chaperone. *Photosynthesis Research* **75**: 11-27.

Quick WP, Chaves MM, Wendler R, David M, Rodrigues ML, Passaharinho JA, Pereira JS, Adcock MD, Leegood RC, Stitt M. 1992. The effect of water stress on photosynthetic carbon metabolism in four species grown under field conditions. *Plant, Cell and Environment* **15**: 25-35.

Raison JK, Berry JA, Armond PA & Pike CS. 1980. Membrane properties in relation to the adaptation of plants to temperature stress. In 'Adaptation of Plants to Water and High Temperature Stress' (eds. NC Turner & PJ Kramer), pp.261-273. John Wiley & Sons, New York.

Raschke K, Reeseman A. 1986. The midday depression of CO_2 assimilation in leaves of *Arbutus unedo* L.: diurnal changes in photosynthetic capacity related to changes in temperature and humidity. *Planta* **168**: 546-503.

Reich PB, Sendall KM, Stefanski A, Wei X, Rich RL, Montgomery RA. 2016. Boreal and temperate trees show strong acclimation of respiration to warming. *Nature* **531**: 633-636.

Rennenberg H, Loreto F, Polle A, Brilli F, Fares S, Beniwal RS, Gessler A. 2006. Physiological responses of forest trees to heat and drought. *Plant Biology* **8:** 556-571.

Rogers A, Medlyn BE, Dukes JS, Bonan G, von Caemmerer S, Dietze MC, Kattge J, Leaky ADB, Mercado LM, Niinemets Ü, Prentice IC, Serbin SP, Sitch S, Way DA, Zaehle S. 2017. A roadmap for improving the representation of photosynthesis in Earth system models. *New Phytologist* **213**: 22-42.

Safronov O, Kreuzwieser J, Haberer G, Alyousif MS, Schulze W, Al-Harbi N, Arab L, Ache P, Stempfl T, Kruse J, Mayer KX, Hedrich R, Rennenberg H, Salojärvi J, Kangasjärvi J. 2017. Detecting early signs of heat and drought stress in *Phoenix dactylifera* (date palm). *PLoS ONE* **12**: e0177883.

This article is protected by copyright. All rights reserved.

Sage RF & Kubien DS. 2007. The temperature response of C_3 and C_4 photosynthesis. *Plant, Cell and Environment* **30**: 1086-1106.

Salvucci ME, Crafts-Brandner SJ. 2004. Relationship between the heat tolerance of photosynthesis and the thermal stability of Rubisco activase in plants from contrasting thermal environments. *Plant Physiology* **134**: 1460-1470.

Schrader SM, Wise RR, Wacholtz WF, Ort DR, Sharkey TD. 2004. Thylakoid membrane responses to moderately high leaf temperature. *Plant, Cell and Environment* **27**: 725-735.

Schulze ED. 1986. Carbon dioxide and water vapor exchange in response to drought in the atmosphere and in the soil. *Annual Review of Plant Physiology and Plant Molecular Biology* **37**: 247-274.

Sharkey TD. 2005. Effects of moderate heat stress on photosynthesis: importance of thylakoid reactions, rubisco deactivation, reactive oxygen species, and thermotolerance provided by isoprene. *Plant, Cell and Environment* **28**: 269-277.

Silim S, Ryan N, Kubien D. 2010. Temperature responses of photosynthesis and respiration in *Populus balsamifera* L.: acclimation versus adaptation. *Photosynthesis Research* **104**: 19-30.

Slot M, Winter K. 2017. *In situ* temperature response of photosynthesis of 42 tree and liana species in the canopy of two Panamanian lowland tropical forests with contrasting rainfall regimes. *New Phytologist* **214**: 1103-1117.

Tcherkez G, Gauthier P, Buckley TN, Busch FA, Barbour MM, Bruhn D, Heskel MA, Gong XY, Crous KY, Griffin K, Way D, Turnbull M, Adams MA, Atkin OK, Farquhar GD, Cornic G. 2017. Leaf day respiration: low CO_2 flux but high significance for metabolism and carbon balance. *New Phytologist* **216**: 986-1001.

Tengberg M. 2003. Research into the origins of date palm domestication. *In:* The date palm: from traditional resource to Green Wealth. *Abu Dhabi* UEA: The Emirates Center for Strategic Studies and Research, 51–62.

Tezara W, Mitchell VJ, Driscoll SD, Lawlor DW. 1999. Water stress inhibits plant photosynthesis by decreasing coupling factor and ATP. *Nature* **401**: 914-917.

Vårhammer A, Wallin G, McLean CM, Dusenge ME, Medlyn BE, Hasper TB, Nsabimana D, Uddling J. 2015. Photosynthetic temperature responses of tree species in Rwanda: evidence of pronounced negative effects of high temperature in montane rainforest climax species. *New Phytologist* **206**: 1000-1012.

Warren CR, Dreyer E. 2006. Temperature response of photosynthesis and internal conductance to CO_2: results from two independent approaches. *Journal of Experimental Botany* **57**: 3057-3067.

This article is protected by copyright. All rights reserved.

Warren CR. 2008. Does growth temperature affect temperature responses of photosynthesis and internal conductance to CO_2? A test with *Eucalyptus regnans*. *Tree Physiology* **28**: 11-19.

Way DA & Sage RF. 2008. Temperature response of photosynthesis in black spruce [*Picea mariana* (Mill.) B.S.P.]. *Plant, Cell and Environment* **31**: 1250-1262.

Way DA, Oren R. 2010. Differential responses to changes in growth temperature between trees from different functional groups and biomes: a review and synthesis of data. *Tree Physiology* **30**: 669-688.

Way DA, Yamori W. 2014. Thermal acclimation of photosynthesis: on the importance of adjusting our definitions and accounting for thermal acclimation of respiration. *Photosynthesis Research* **119**: 89-100.

Wong SC, Cowan IR, Farquhar GD. 1979. Stomatal conductance correlates with photosynthetic capacity. *Nature* **282**: 424-426.

Wong SC, Cowan IR, Farquhar GD. 1985. Leaf conductance in relation to rate of CO_2 assimilation. II. Effects of short-term exposures to different photon flux densities. *Plant Physiology* **78**: 826-829.

Wright IJ, Dong N, Maire V, Prentice C, Westoby M, Díaz S, Gallagher RV, Jacobs BF, Kooymann R, Law EA, Leishmann MR, Niinemets Ü, Reich PB, Sack L, Villar R, Wang H, Wilf P. 2017. Global climatic drivers of leaf size. *Science* **357**: 917-921.

Xu L, Baldocchi DD. 2003. Seasonal trends in photosynthetic parameters and stomatal conductance of blue oak (*Quercus douglasii*) under prolonged summer drought and high temperature. *Tree Physiology* **23**: 865-877.

Yamori W, Noguchi K, Hanba YT, Terashima I. 2006. Effects of internal conductance on the temperature dependence of the photosynthetic rate in spinach leaves from contrasting growth temperatures. *Plant Cell Physiology* **47**: 1069-1080.

Yamori W, Noguchi K, Kashino Y, Terashima I. 2008. The role of electron transport in determining the temperature dependence of the temperature dependence of the photosynthetic leaves in spinach leaves grown at contrasting temperatures. *Plant Cell Physiology* **49**: 583-591.

Yamori W, Hikosaka K, Way DA. 2014. Temperature response of photosynthesis in C_3, C_4 and CAM plants: temperature acclimation and temperature adaptation. *Photosynthesis Research* **119**: 101-117.

Zhu X-G, de Sturler E, Long SP. 2007. Optimizing the distribution of resources between enzymes of carbon metabolism can dramatically increase photosynthetic rate: a numerical simulation using an evolutionary algorithm. *Plant Physiology* **145**: 513-526.

This article is protected by copyright. All rights reserved.

Accepted Article

Accepted Article

Supporting Information

Additional Supporting Information may be found online in the Supporting Information section at the end of the article:

Dataset S1. Raw data collected during the experiment.

Notes S1. Description of variables in the dataset S1.

Fig. S1 Growth facilities at the Helmholtz Centre in Munich.

Fig. S2 Between-day record of meteorological conditions within the experimental period.

Fig. S3 Biometric data of date palm seedlings (aboveground biomass, LMA and leaf-N).

Fig. S4 Instantaneous temperature resonses of leaf gas exchange, fitted to a three-parameter extended Arrhenius equation.

Fig. S5 Intrinsic water use efficiency of leaf photosynthesis at T_{opt} and $\delta^{13}C$ –signature of leaves.

Fig. S6 Rates of leaf dark respiration at 39°C measurement temperature (R_{39}).

Fig. S7 Dependency of either δ_A or δ_G on three principal continuous variables.

Fig. S8 Sensitivity of stomatal conductance towards leaf net photosynthesis relative to vapour pressure deficit.

Fig. S9 Treatment effects on g_1*.

Table S1. Experimental setup to test for the effects of season and daily irrigation regime on gas exchange of date palm.

Table S2. Parameter values derived from individual A-T and G-T responses, fitted to the extended Arrhenius- equation.

Table S3. General Linear Models using a mixture of predictor continuous variables to test for the effects on either δ_A or δ_G.

Figure captions:

Figure 1. Meteorological conditions during a typical winter and summer day in Saudi Arabia. **(a)** Diurnal variation in ambient air temperature. **(b)** Diurnal variation in vapour pressure deficit (VPD). **(c)** Diurnal variation in photosynthetic active radiation (PAR). Grey bars in (a) and (b) show SE. Gas exchange measurements were conducted in the morning (7:45am-11:00am), at midday (11:00am -14:15pm) and in the afternoon (14:15-17:30pm). Meteorological conditions were maintained throughout the entire experimental period (Supporting Information, Fig. S2).

This article is protected by copyright. All rights reserved.

Figure 2. Soil water content over the course of the experiment, as affected by irrigation regime and season. Data shown are averages ± SE.

Figure 3. Instantaneous temperature responses of leaf gas exchange in *Phoenix dactylifera*. **(a-d)** Temperature responses of net leaf CO_2-assimilation (*A*) during acclimation to differing season and soil water availability. **(e-h)** Temperature responses of stomatal conductance (*G*) during acclimation to differing season and soil water availability. Data shown are averages ± SE of 11-12 independent replicates. Closed circles, winter, $+H_2O$; open circles, winter, $-H_2O$; closed triangles, summer, $+H_2O$; open triangles, summer, $-H_2O$. Data were subsequently $\log_e$-transformed (see Eqn. 2) and plotted against reciprocal temperature, as shown in Supporting Information Fig. S4.

Figure 4. Intrinsic leaf water use efficiency (WUE_i) during acclimation to differing season and soil water availability in *Phoenix dactylifera*. **(a-d)** Temperature responses of intrinsic water use efficiency ($WUE_i = A/G$) during the course of the experiment. **(e-h)** Temperature responses of C_i/C_a during the course of the experiment. Data shown are averages ± SE of 11-12 independent replicates. Closed circles, winter, $+H_2O$; open circles, winter, $-H_2O$; closed triangles, summer, $+H_2O$; open triangles, summer, $-H_2O$.

Figure 5. Leaf photosynthesis and water use efficiency at optimum temperature in *Phoenix dactylifera*. **(a-d)** Treatment effects on optimum temperature (T_{opt}), where peak rates of photosynthesis were recorded. **(e-h)** Treatment effects on rates of photosynthesis at optimum temperature (A_{opt}). **(i-l)** Treatment effects on intrinsic water use efficiency at optimum temperature ($WUE_i = A_{opt}/G_{opt}$). Columns show averages ± SE of 3-4 independent replicates. Columns are aligned to represent measurements in the morning, at midday, and in the afternoon (refer also to Fig. 1). Black columns, winter, $+H_2O$; dark grey columns, winter, $-H_2O$; light grey columns, summer, $+H_2O$; open columns, summer, $-H_2O$. Data were subjected to 3-way ANOVA, to test for principal treatment effects within respective measurement periods. S, effect of season; W, effect of irrigation regime; D, time- of- measurement effect (day time). *, significant at $p< 0.05$; ns, not significant. For further results of ANOVA, see Table 2.

Figure 6. Acclimation of leaf gas exchange to ambient temperature and water availability in *Phoenix dactylifera*. **(a)** Relation between optimum temperature of leaf photosynthesis (T_{opt}) and ambient temperature within growth cabinets (T_{growth}). T_{growth} denotes air temperature prior to start of measurements. T_{opt} denotes leaf temperature under cuvette measuring conditions (PAR: 1500 µmol m^{-2} s^{-1}; air flow: 700 µmol s^{-1}; well- stirred air using impellers). **(b)**

This article is protected by copyright. All rights reserved.

Accepted Article

Relation between T_{opt}, at which peak rates of *A* were recorded, and 'equilibrium temperature' ($T_{equ.}$), at which *A*/*G* is insensitive to small variation in measurement temperature (and C_i/C_a is constant). T_{opt} was determined via Eqn. 3, and $T_{equ.}$ via Eqn. 6. Closed black symbols, winter, $+H_2O$; open black symbols, winter, $-H_2O$; closed grey symbols, summer, $+H_2O$; open grey symbols, summer, $-H_2O$. Upper triangles, morning; squares, midday; lower triangles, afternoon. Blue circles, winter, recovery; red circles, summer, recovery. Data show averages ± SE of 15-16 replicates for fully watered plants (closed symbols), 7- 8 replicates for water-deprived plants (i.e., during T2 + T3, open symbols), and 12 replicates for recovery treatments (averaged across day times, coloured circles)**.** For further statistical analysis of results, see Fig. 7.

Figure 7. Contrast between key temperatures set by the physiology of leaf gas exchange in *Phoenix dactylifera*. **(a-c)** Difference between T_{opt} and T_{growth} in response to seasonal 'climate' (a), irrigation regime (b) and day time (c). **(d-f)** Difference between T_{equ} and T_{opt} in response to principal treatments. T_{growth} denotes growth temperature (°C, air temperature in growth cabinets prior to measurements), T_{opt} denotes optimum temperature of leaf photosynthesis (°C, leaf temperature under cuvette measuring conditions), and T_{equ} denotes equilibrium temperature (°C, leaf temperature at which sub-stomatal CO_2-concentration (C_i) is insensitive to small temperature changes). Columns show averages ±SE. Replicate number for individual columns are shown at the bottom of each panel. Different letters indicate significant differences between means ($p < 0.05$; post-hoc HSD Tukey test for dissimilar replicate number).

Figure 8. Relation between two exponent parameters of an extended Arrhenius equation that capture (instantaneous) temperature sensitivities of photosynthesis and stomatal conductance in *Phoenix dactylifera*. **(a)** Correlation between $\mu_{Ref.A}$ and δ_A. $\mu_{Ref.A}$ defines the slope of ln*A* (or the activation energy of *A*) at the reference temperature (i.e., at 294K (=21°C)), and δ_A describes dynamic change in activation energy of *A* as leaf temperature increases. **(b)** Correlation between $\mu_{Ref.G}$ and δ_G. $\mu_{Ref.G}$ defines the slope of ln*G* at the reference temperature, and δ_G describes the shape or 'curvature' of G-T response, i.e. the dynamic change in activation energy of *G* as leaf temperature increases. Closed black symbols, winter, $+H_2O$ (including recovery); open black symbols, winter, $-H_2O$; closed grey symbols, summer, $+H_2O$ (including recovery); open grey symbols, summer, $-H_2O$. Upper triangles, morning; squares, midday; lower triangles, afternoon. Additional influences on the relation between respective exponent parameters (i.e., sources of residual variation) were identified and quantified via General Linear Models (see Supporting Information Table S3 and Fig. S7).

Figure 9. Stomatal conductance and evapotranspiration of *Phoenix dactylifera* leaves, as affected by vapour pressure deficit (VPD). **(a-d)** Sensitivity of steady- state stomatal conductance (*G*) to vapour pressure deficit experienced by leaves during measurements. **(e-h)**

This article is protected by copyright. All rights reserved.

Accepted Article

Leaf evapotranspiration (*E*), as driven by *G* and VPD during measurements. Data shown are averages ± SE of 11-12 independent replicates. Closed circles, winter, $+H_2O$; open circles, winter, $-H_2O$; closed triangles, summer, $+H_2O$; open triangles, summer, $-H_2O$.

Accepted Article

This article is protected by copyright. All rights reserved.

Table 1 Results of analysis of variance.

(a)		Source of variation					
		Season (S)		Watering regime (W)		Time of day (D)	
		$_p\eta^2$	P-value	$_p\eta^2$	P-value	$_p\eta^2$	P-value
T1: Temperture acclimation	T_{opt}	**0.58**	<0.001	-	-	**0.43**	<0.01
	A_{opt}	**0.47**	<0.001	-	-	0.16	0.20
	WUE_i (at T_{opt})	0.17	0.06	-	-	0.05	0.66
T2: Mild drought	T_{opt}	**0.56**	<0.001	0.01	0.57	**0.20**	0.02
	A_{opt}	**0.29**	<0.001	**0.12**	0.03	0.02	0.65
	WUE_i (at T_{opt})	0.02	0.45	0.07	0.12	0.02	0.73
T3: Severe drought	T_{opt}	**0.58**	<0.001	0.04	0.25	**0.19**	0.02
	A_{opt}	0.02	0.40	**0.50**	<0.001	**0.25**	<0.01
	WUE_i (at T_{opt})	0.02	0.48	**0.21**	<0.01	0.04	0.48
T4: Recovery	T_{opt}	**0.69**	<0.001	0.03	0.31	**0.31**	<0.01
	A_{opt}	**0.20**	<0.01	0.01	0.56	0.04	0.52
	WUE_i (at T_{opt})	0.01	0.50	0.01	0.71	0.06	0.34
(b)		Season (S)		Watering regime ($W^{\#}$)		Time of day (D)	
		$_p\eta^2$	P-value	$_p\eta^2$	P-value	$_p\eta^2$	P-value
T1-T4[#]	T_{opt}	**0.52**	<0.001	**0.07**	<0.01	**0.18**	<0.001
	A_{opt}	**0.11**	<0.001	**0.24**	<0.001	**0.08**	<0.01
	WUE_i (at T_{opt})	**0.03**	<0.05	**0.09**	<0.001	0.01[a]	0.37
	[b]R_{39}	**0.13**	<0.001	**0.05**	<0.01	**0.17**	<0.001

Data were subjected to 3-way ANOVA, to test for effects of differing season, watering regime and day time on T_{opt}, A_{opt} and WUE_i in *Phoenix dactylifera*. T_{opt} denotes optimum temperature of leaf net photosynthesis (°C, leaf temperature under cuvette measuring conditions), A_{opt} denotes peak rates of leaf net photosyntheis at T_{opt} (µmol m^{-2} s^{-1}), WUE_i denotes intrinsic water use efficiency at T_{opt} ($WUE_i = A_{opt}/G_{opt}$, µmol mol^{-1}) and R_{39} denotes rates of leaf dark respiration (µmol m^{-2} s^{-1}) at 39°C measurement temperature. **(a)** Treatment effects within respective measuring periods (T1, T2, T3, T4). **(b)** Treatment effects over the entire experimental period (T1-T4). In this analysis, data obtained from water- deprived plants during T2+T3 were assigned to a $-H_2O$ treatment, and the recovery treatment (T4) was added the $+H_2O$ treatment (i.e., watering regime denoted as $W^{\#}$). Data shown are effect sizes ($_p\eta^2$) and corresponding P-values. Effect sizes in bold font are significant at $P< 0.05$. [a]significant $W^{\#}$×D- effect ($_p\eta^2$: 0.06; $P< 0.01$). [b]Results for R_{39} are shown in Supporting Information, Fig. S6.

This article is protected by copyright. All rights reserved.

Table 2. Effects of season and drought on parameters describing the temperature sensitivity of leaf photosynthesis (*A*) and stomatal conductance (*G*) in *Phoenix dactylifera*.

	Treatment				Source of variation			
	Winter	Winter	Summer	Summer	Season (S)		Water regime (W)	
	+H_2O	-H_2O	+H_2O	-H_2O	${}_p\eta^2$	P-value	${}_p\eta^2$	P-value
$\mu_{Ref.A}$ (kK)	13.2±2.3	12.2±3.1	27.8±3.6	17.7±3.1	**0.11**	0.001	0.02	0.07
δ_A (kK^2)	-88±8	-103±13	-88±10	-53±11	**0.06**	0.02	0.01[a]	0.37
lnA_{opt} (µmol m^{-2} s^{-1})	1.2±0.1	0.4±0.2	1.8±0.1	0.8±0.2	**0.09**	0.003	**0.23**	<0.001
$\mu_{Ref.G}$ (kK)	5.5±1.1	0.9±1.3	16.9±1.7	7.2±1.8	**0.28**	<0.001	**0.20**	<0.001
δ_G (kK^2)	-37±3	-15±4	-51±5	-22±6	**0.05**	0.03	**0.23**	<0.001
lnG_{ref} (mmol m^{-2} s^{-1})	3.2±0.2	2.8±0.1	2.3±0.2	2.5±0.2	**0.11**	0.001	0.002	0.67

The meaning of exponent parameters μ_{Ref} and δ is explained in the caption of Fig. 8. lnA_{opt} denotes $\log_e$- transformed rates of photosynthesis at optimum temperature, and lnG_{ref} denotes $\log_e$- transformed stomatal conductance at reference temperature (also see Supporting Information Table S3 and Fig. S7). Data shown on the left-hand side of Table 2 show averages ± SE of 23-24 replicates (i.e., data from T2 + T3). Data were subjected to 2-way ANOVA (omitting the effect of day time). Data on the right hand side show principal effects of season and irrigation regime on parameter values. Effect sizes (${}_p\eta^2$) in bold font are significant at $P< 0.05$. [a]significant S*W- effect (${}_p\eta^2 = 0.05$; $P= 0.03$).

This article is protected by copyright. All rights reserved.

Accepted Article

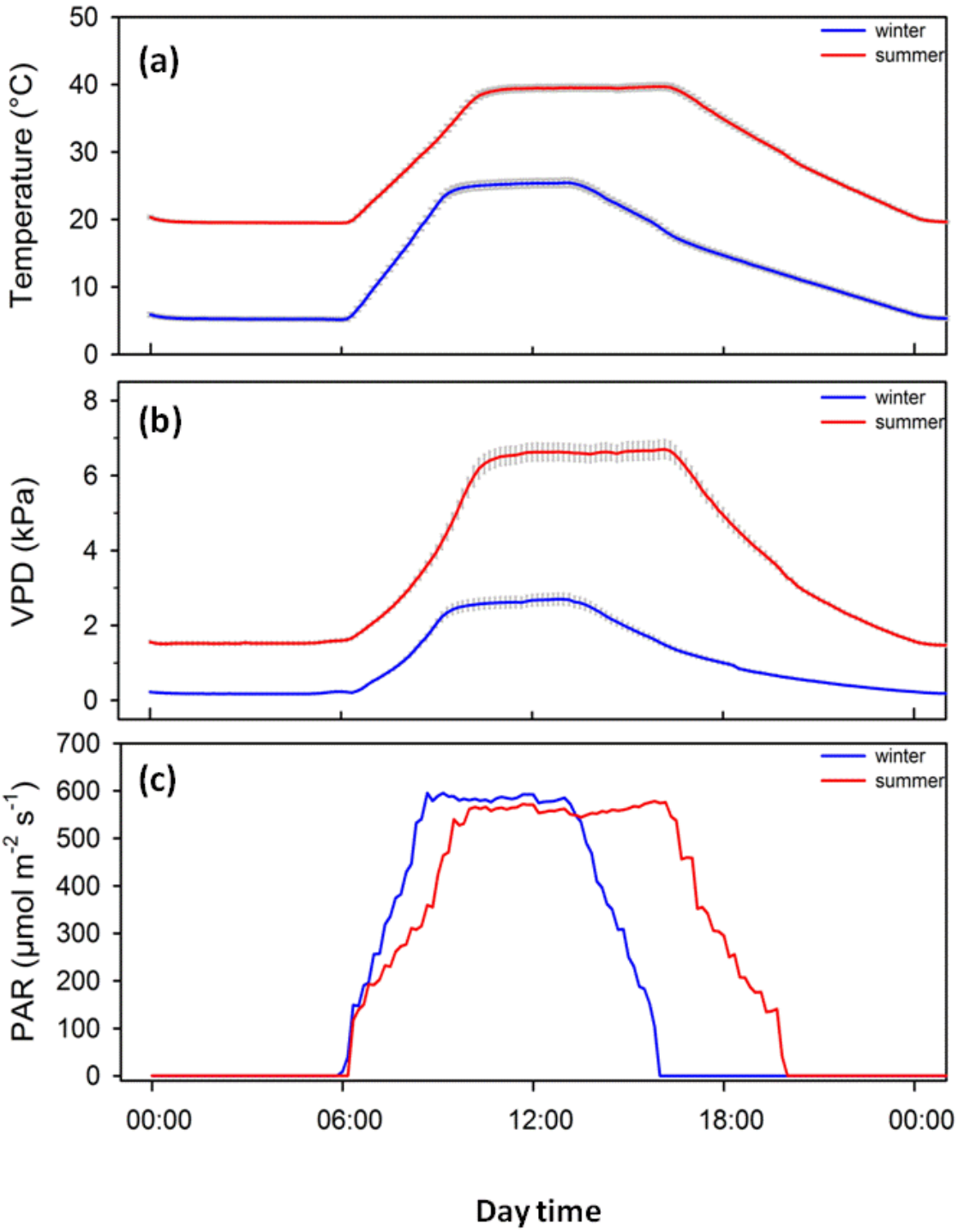

This article is protected by copyright. All rights reserved.

Accepted Article

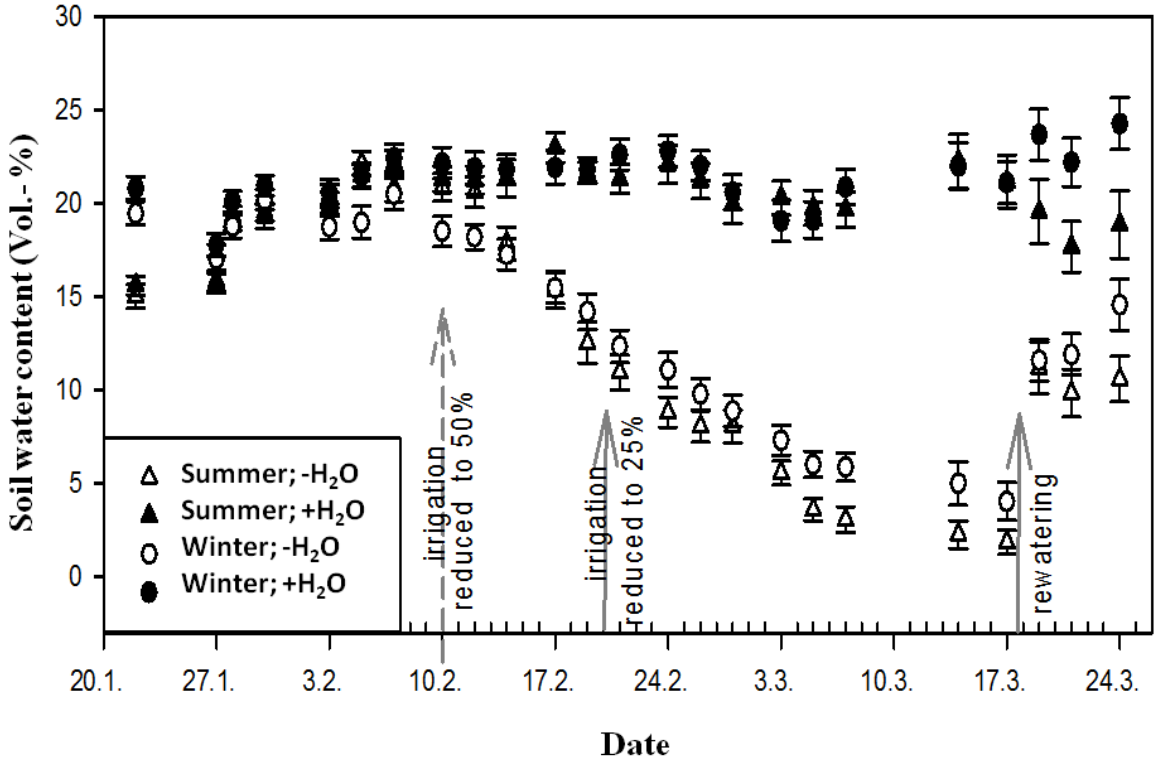

This article is protected by copyright. All rights reserved.

Accepted Article

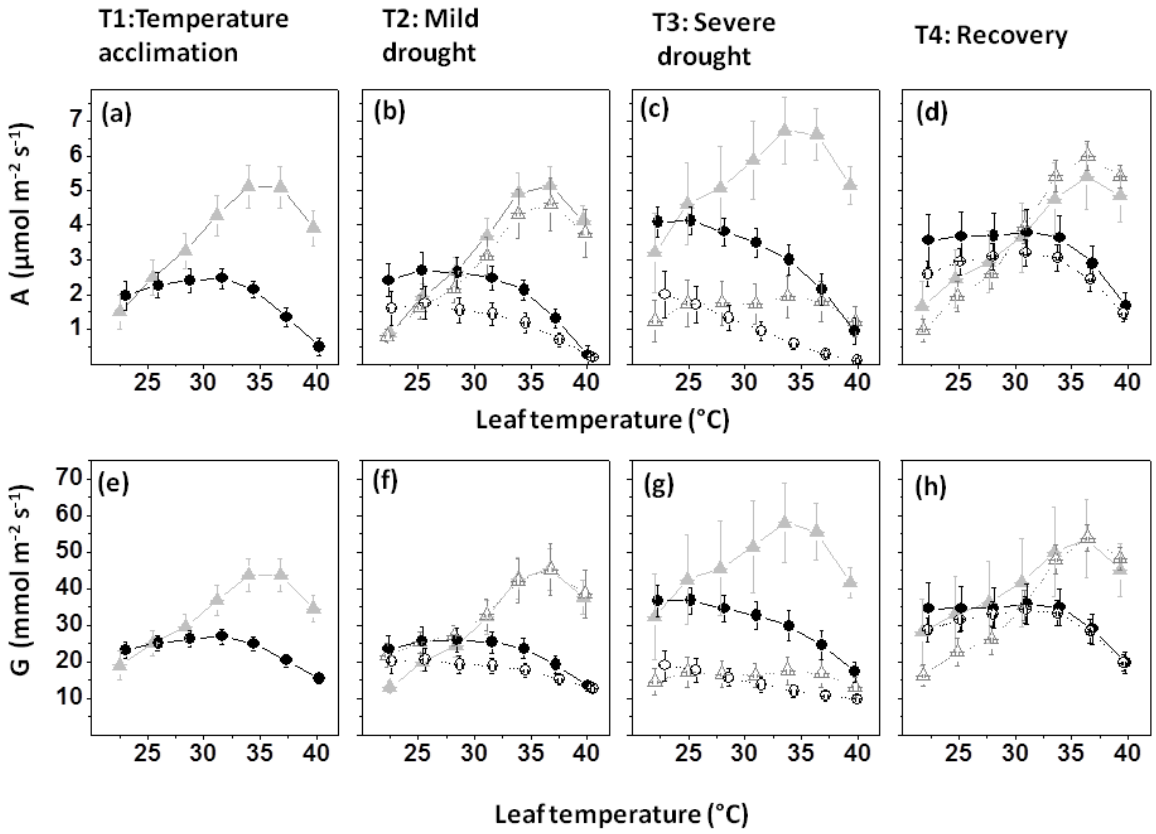

This article is protected by copyright. All rights reserved.

Accepted Article

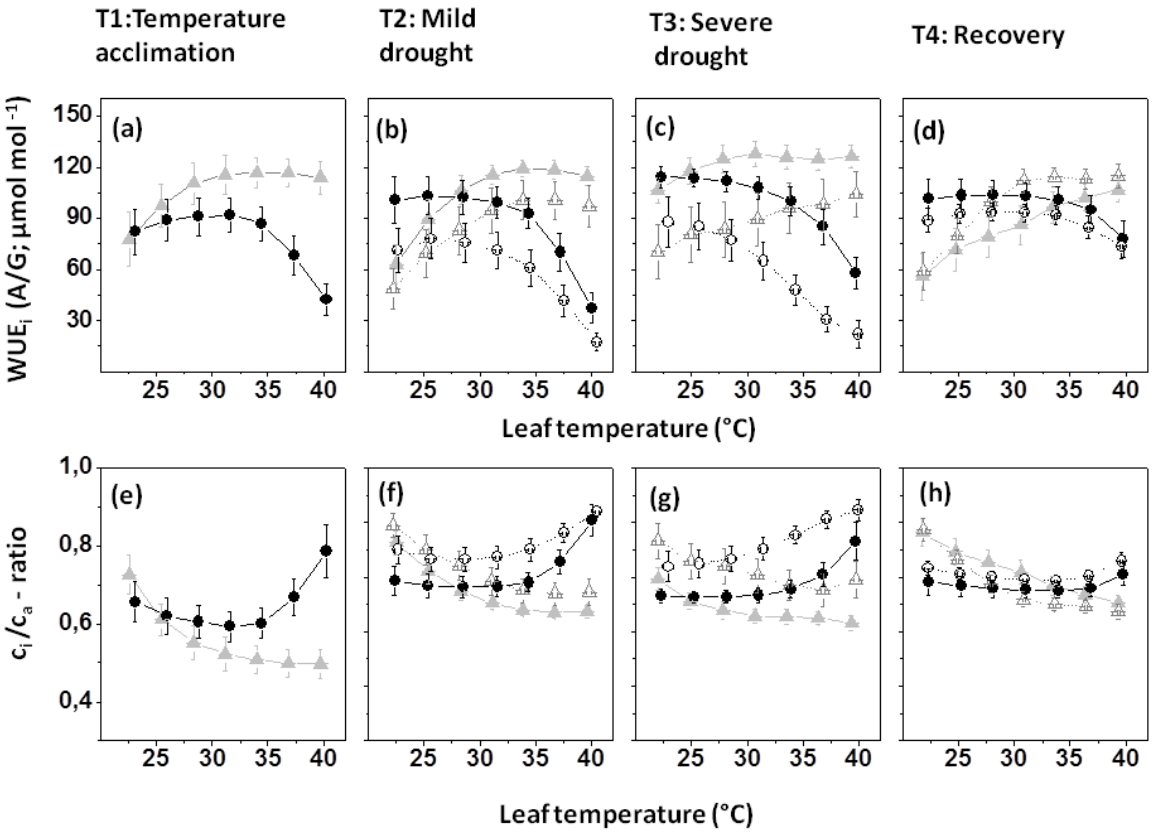

This article is protected by copyright. All rights reserved.

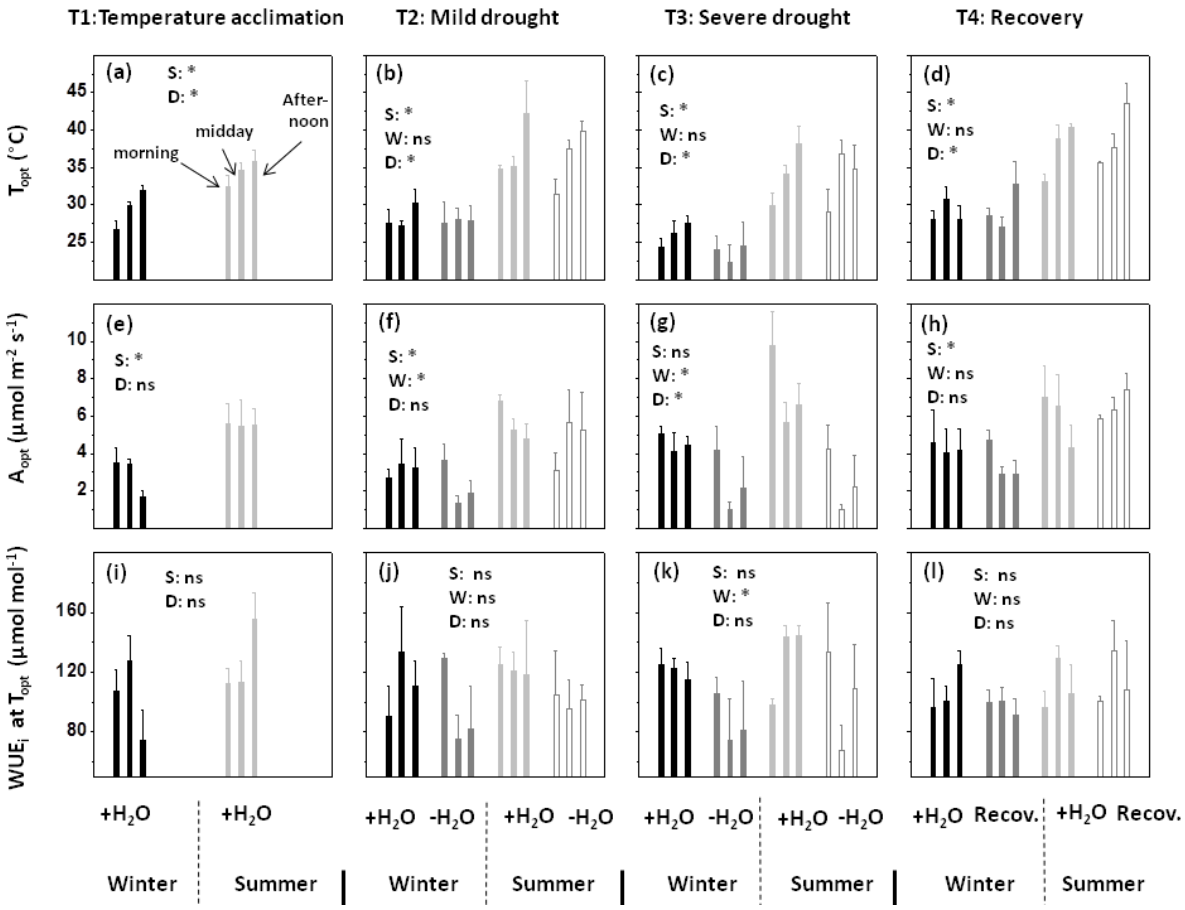

Accepted Article

This article is protected by copyright. All rights reserved.

Accepted Article

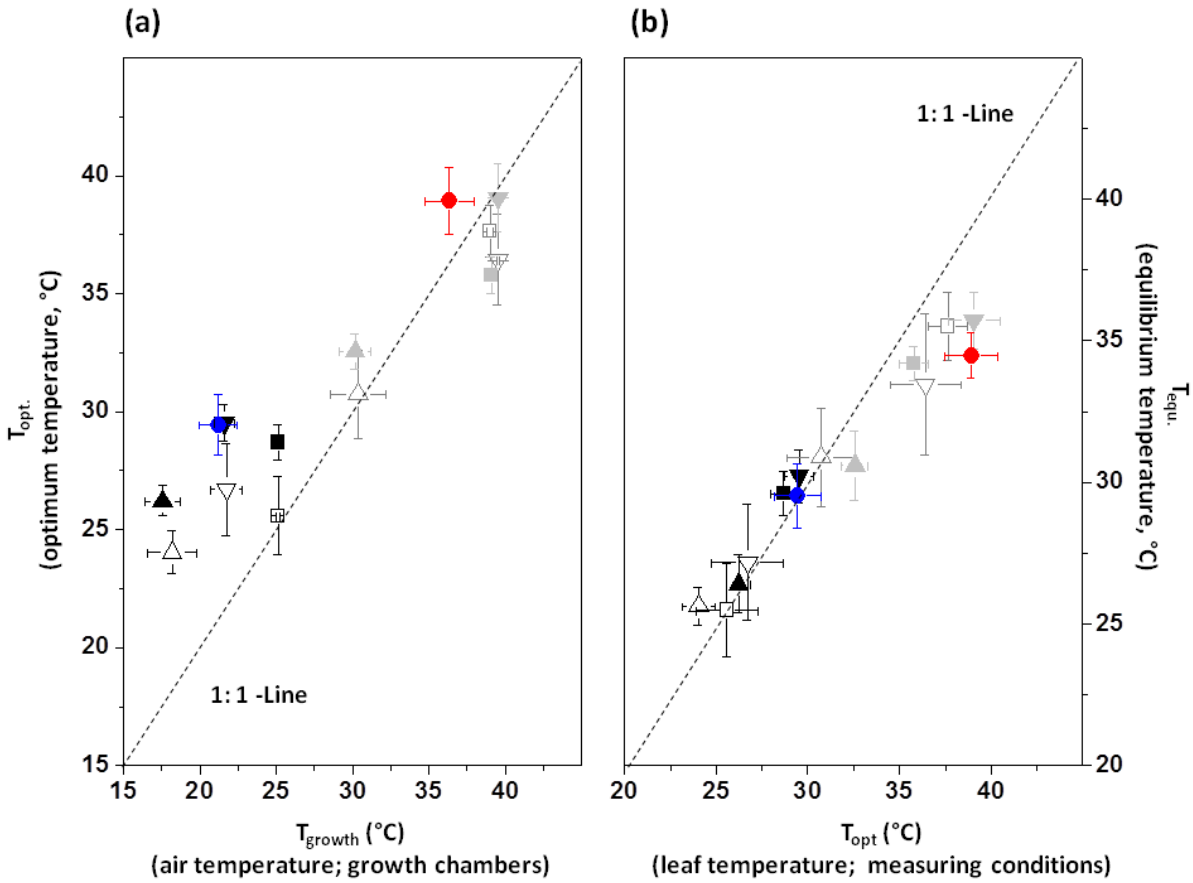

This article is protected by copyright. All rights reserved.

Accepted Article

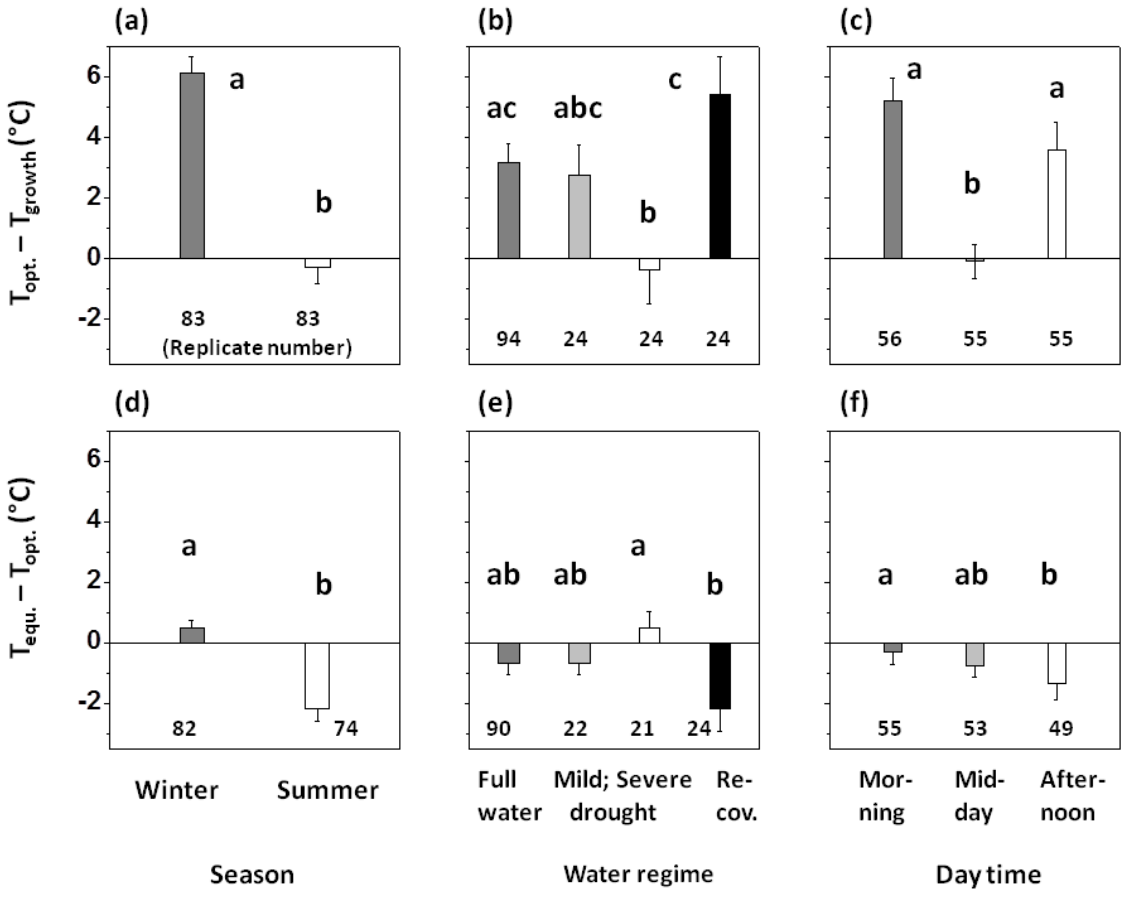

This article is protected by copyright. All rights reserved.

Accepted Article

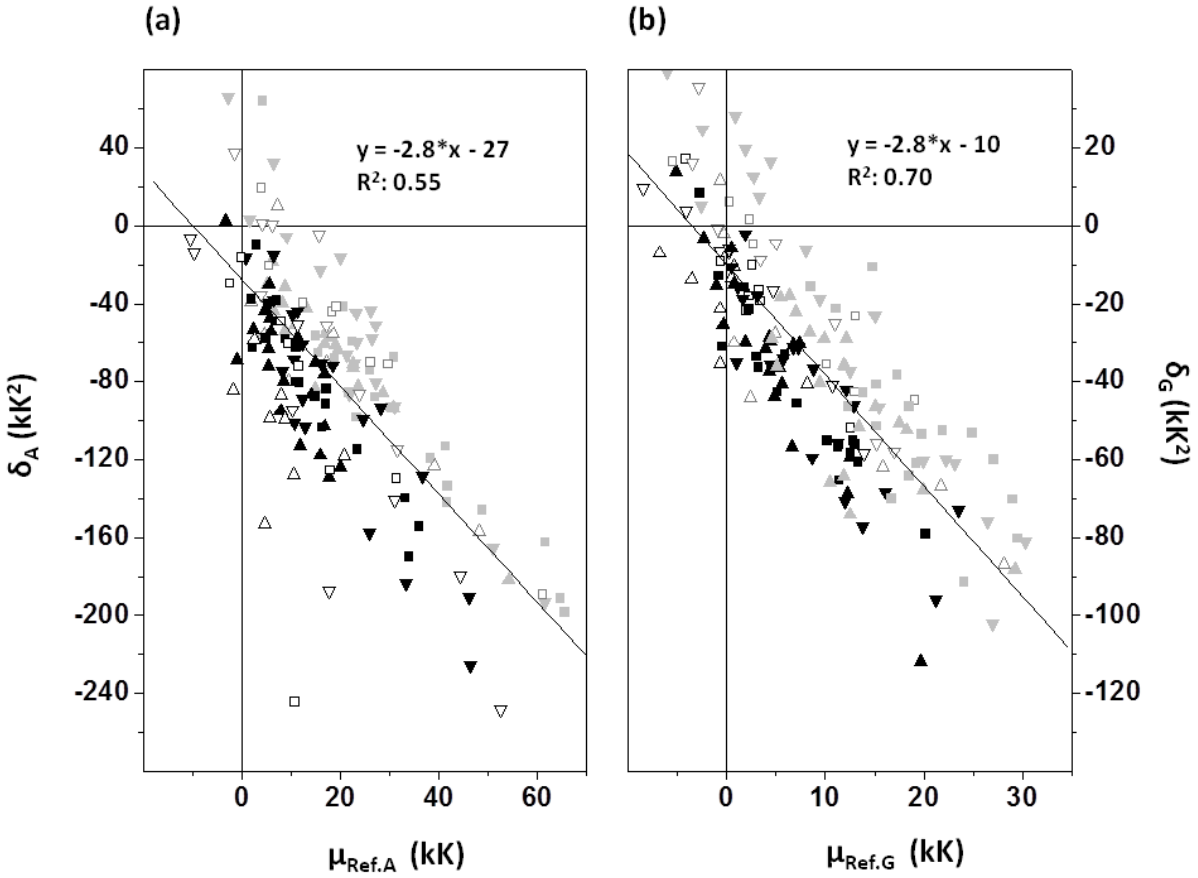

This article is protected by copyright. All rights reserved.

Accepted Article

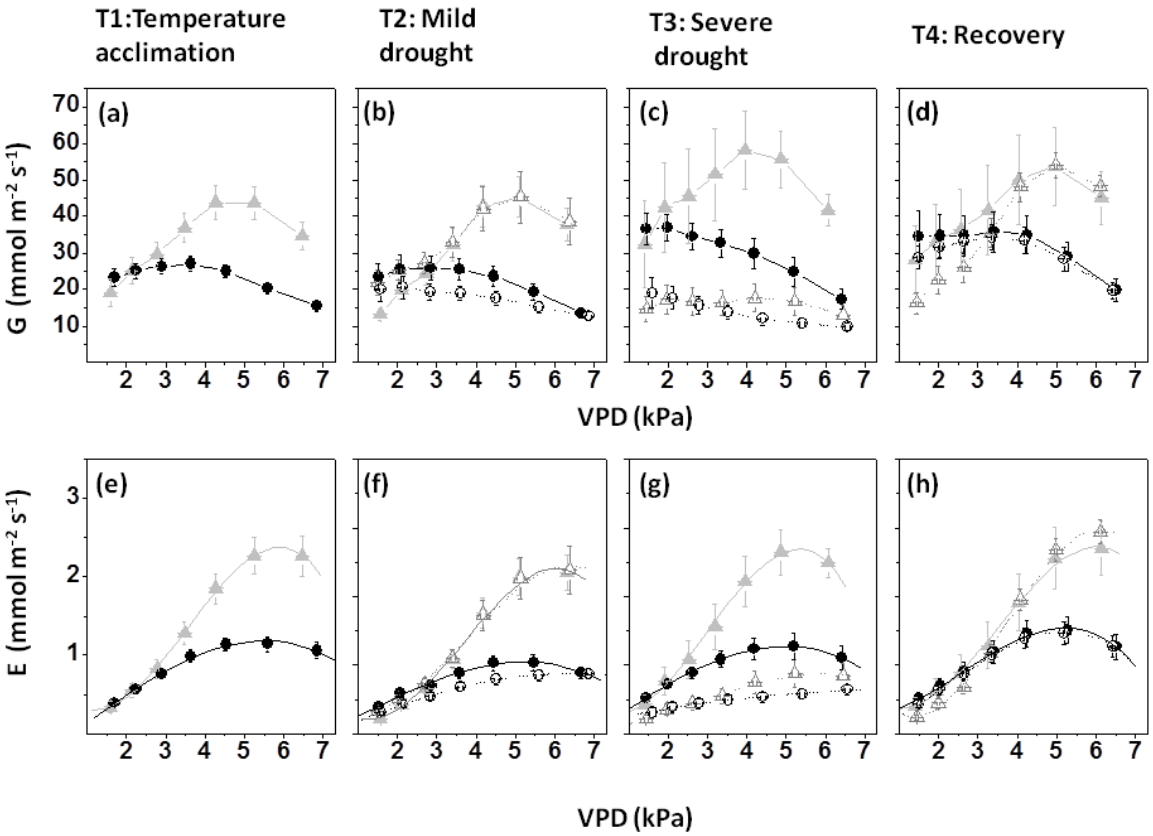

This article is protected by copyright. All rights reserved.